Manaaki Whenua
Landcare Research

SedNetNZ modelling for freshwater planning in Otago

Prepared for: Otago Regional Council

February 2022

SedNetNZ modelling for freshwater planning in Otago

Contract Report: LC5016

Andrew Neverman, Hugh Smith

Manaaki Whenua – Landcare Research

Reviewed by:	*Approved for release by:*
Chris Phillips Senior Researcher Manaaki Whenua – Landcare Research	John Triantafilis Portfolio Leader – Managing Land & Water Manaaki Whenua – Landcare Research

Contents

Summary v

1 Introduction 1

2 Background 1

3 Objectives 2

4 Methods 2

4.1 SedNetNZ Model Description 2

4.2 Selecting monitoring sites for analysis 10

4.3 Application of SedNetNZ to Otago 14

4.4 Model simulations 14

4.5 Future attribute states 20

5 Results 21

5.1 Sediment loads 21

5.2 Achievement of NOF attribute states 25

6 Discussion 31

6.1 Effectiveness of aspirational mitigations 31

6.2 Improving NOF attribute state 32

6.3 Model assumptions and limitations 33

7 Conclusions 36

8 Recommendations 37

9 Acknowledgements 37

10 References 37

Summary

Project and Client

- Otago Regional Council (ORC) contracted Manaaki Whenua – Landcare Research (MWLR) to model mean annual suspended sediment loads and the reductions in load required to meet the suspended fine sediment attribute states (visual clarity) in the National Policy Statement for Freshwater Management 2020 amendment (NPS-FM 2020) at selected State of the Environment (SoE) monitoring sites. This modelling will contribute to freshwater objectives setting in the Otago region.

Objectives

- Using SedNetNZ, model mean annual suspended sediment loads at SoE monitoring sites for:
  - a scenario representing the contemporary land cover with baseline erosion mitigation.
  - a scenario representing contemporary land cover with implementation of aspirational erosion mitigation practices, representing a potential upper limit of achievable sediment load reductions.
- Model the reductions in contemporary mean annual suspended sediment loads required to achieve the national bottom line and A-C attribute states for suspended fine sediment in the NPS-FM 2020.
- Assess the achievable attribute state of SoE sites through implementation of aspirational erosion mitigation practices.

Methods

- Mean annual suspended sediment loads were modelled for a nominal year of 2017 to represent contemporary mean annual suspended sediment loads using the 2018 landcover from the New Zealand Landcover Database version 5 (LCDB), the extent of winter forage cropping as mapped by Belliss et al. (2019), and an estimate of the extent of existing riparian fencing on mitigatable land based on results from the 2017 Survey of Rural Decision Makers (SRDM) (Stahlmann-Brown 2021).
- A future aspirational scenario was modelled with a completed extent of riparian fencing (i.e. all mitigatable riparian land fenced) with a 3-m buffer. This scenario represents the maximum potential load reductions achievable given full implementation and maturity of these mitigations in Otago and can be used to assess the feasibility of achieving suspended fine sediment attribute states under the NPS-FM 2020.
- Baseline visual clarity for SoE monitoring sites (n = 116) across the Otago region were provided by ORC. 55 sites did not have monitoring records of sufficient length to derive a baseline (5 years of data required by NPS-FM 2020 for suspended fine sediment baseline). Of the 61 sites with 5 years of data, 27 were compliant with band A, and are therefore unable to achieve a higher attribute state so are not assessed for load reductions in this report. 34 SoE sites had a baseline attribute state below band A. The mean annual suspended sediment load reductions required to achieve higher attribute

states were calculated for these 34 sites using national-scale empirical models of the relationship between suspended sediment concentration (SSC) and visual clarity.

Results

- In total, 489 kt yr^{-1} of suspended sediment was estimated to reach coastal receiving environments in Otago under the baseline scenario.
- Implementation of aspirational erosion mitigations achieved a 28% reduction in suspended sediment load that resulted in 351 kt yr^{-1} reaching coastal receiving environments.
- 12 of the 24 (50%) SoE sites with a baseline attribute state in the D band are brought above the national bottom line in the aspirational scenario. In total, 49 of 61 sites (80%) comply with the national bottom line under the aspirational scenario.
- Improvements in attribute state are seen at 22 of the 34 SoE sites (65%) in the aspirational scenario.
- Under the aspirational scenario the number of sites achieving band A increases from 27 to 33, and from 3 to 9 for band B.

Conclusions and Recommendations

- SedNetNZ modelling showed that widespread implementation of riparian fencing reduced mean annual suspended sediment loads and increased the number of SoE sites exceeding national bottom line and meeting the attribute state for bands A and B.
- Not all SoE sites achieve the national bottom line under the aspirational scenario. Most of these sites occur in the Manuherikia and Taieri catchments. Visual clarity in these catchments may be affected by naturally occurring dissolved organic matter, such as tannins, and may not be directly attributable to suspended sediment. In such cases, visual clarity objectives may need to be set below the national bottom line in accordance with exemptions for naturally occurring processes in the NPS-FM 2020.
- The SedNetNZ modelling did not account for the effects of climate change in the region. Future suspended sediment load modelling could include representation of the potential impacts of climate change on the achievability of attribute states.
- Acquisition of spatial data on the extent of existing riparian fencing across the region would enable a) better parameterisation of the baseline scenario, and b) more accurate estimation of the remaining length of streams to be fenced under future mitigation scenarios.
- Use of LiDAR data would support improved representation of erosion processes. SedNetNZ modelling could be updated when LiDAR data become available for the Otago region.
- Further investigation into the potential contribution of dissolved organic matter to low visual clarity (high turbidity) at SoE sites in the Otago region would assist with setting feasible visual clarity objectives.

1 Introduction

The environmental effects of activities affecting water bodies are primarily managed through the Regional Plan: Water in the Otago region. Following amendments to the National Policy Statement for Freshwater Management, which came into effect on 3 September 2020 (NPS-FM 2020), regional plans are required to be amended to include the objectives and policies set out in the NPS-FM 2020.

A suspended fine sediment attribute was added to the National Objectives Framework (NOF) in the NPS-FM 2020, requiring councils to set objectives for suspended fine sediment in their region. Otago Regional Council (ORC) contracted Manaaki Whenua – Landcare Research (MWLR) to use spatial modelling to identify the reductions in suspended sediment loads required to achieve each NOF attribute band at State of the Environment (SoE) monitoring sites. ORC also requested a scenario be modelled to test the potential upper limit of suspended sediment load reductions achievable under widespread implementation of riparian stock exclusion fencing (aspirational scenario), and to assess the NOF attribute states achievable under this scenario at SoE monitoring sites.

SedNetNZ (Dymond et al. 2016) was identified as the most appropriate model for this objective. SedNetNZ is a steady-state sediment budget model designed to represent the diversity of erosion processes that occur in the New Zealand landscape and predict mean annual suspended sediment loads (Dymond et al. 2016). Recent updates to the SedNetNZ model include improved representation of streambank erosion (Smith et al. 2019a) as well as spatial variability in surface soil erodibility and lake trapping of suspended sediment (Neverman et al. 2021a, 2021b). SedNetNZ represents erosion processes individually, allowing direct targeting of erosion processes with appropriate mitigations during scenario modelling. SedNetNZ has been used in other regions, including Southland and Taranaki (Neverman et al. 2021a, 2021b), for similar scenario modelling to assess the achievement of suspended fine sediment objectives related to the NOF.

2 Background

In 2020 the Ministry for the Environment (MfE) amended the National Policy Statement for Freshwater Management (NPS-FM) and National Objectives Framework (NOF). The NPS-FM and NOF require a minimum standard to be achieved (a national bottom line) for water quality attributes, along with a requirement for no further degradation for water bodies which already exceed the national bottom line. Councils are required to develop plans to achieve these standards.

Previous versions of the National Policy Statement for Freshwater Management (NPS-FM 2014 and 2017) did not include limits for suspended fine sediment. Following the 2017 amendment, MfE led work to develop a suspended fine sediment attribute (Franklin et al. 2019; Hicks et al. 2019; Neverman et al. 2019). This work resulted in the inclusion of a suspended fine sediment attribute in the 2020 amendment to the NPS-FM, with attribute states set using visual clarity as the attribute unit.

The basis for relating changes in modelled suspended sediment loads and visual clarity draws on previous work. Dymond et al. (2017) identified a relationship between suspended sediment concentration and visual clarity. Hicks et al. (2019) used this relationship to develop a nationally fitted model to predict the reductions required in mean annual suspended sediment loads to achieve visual clarity objectives. Following Neverman et al. (2021a, 2021b) and Vale et al. (2021), the model developed by Hicks et al. (2019) has been applied to estimate the reductions in SedNetNZ modelled baseline mean annual suspended sediment loads required to achieve the NOF attribute states for suspended fine sediment at SoE monitoring sites across Otago.

3 Objectives

- Using SedNetNZ, model mean annual suspended sediment loads at SoE monitoring sites using for:
    - a scenario representing the contemporary land cover with baseline erosion mitigation.
    - a scenario representing contemporary land cover with implementation of aspirational erosion mitigation practices, representing a potential upper limit of achievable sediment load reductions.
- Model the reductions in contemporary mean annual suspended sediment loads required to achieve the national bottom line and A-C attribute states for suspended fine sediment in the NPS-FM 2020.
- Assess the achievable attribute state of SoE sites through implementation of aspirational erosion mitigation practices.

4 Methods

4.1 SedNetNZ Model Description

4.1.1 Surficial Erosion

Surficial erosion processes in SedNetNZ (Dymond et al. 2016) are represented by the NZUSLE (Dymond 2010) model:

$$ES = a\,P^2 KLSC \qquad (1)$$

where ES denotes surficial erosion in t km^{-2} yr^{-1}; a is a constant (t km^{-2} yr^{-1} mm^{-2}) calibrated against surface erosion rate data from New Zealand (Dymond 2010) with a value of 1.2 x 10^{-3}; P is mean annual rainfall (mm); K is the soil erodibility factor (dimensionless), L is the slope length factor; S is the slope steepness factor; and C represents the impact of vegetation cover (dimensionless) (1.0 for bare ground, 0.01 for pasture, and 0.005 for forest and scrub).

In this study, we use a revised representation of surficial erosion processes as part of the SedNetNZ model. Following Smith et al. (2019b), this includes replacing the uniform slope length factor (*L*) of the NZUSLE (Dymond 2010) with a factor that better represents the effect of topography on the size of convergent upslope areas contributing overland flow and surficial erosion, as described by Desmet and Govers (1996):

$$L = \frac{(A + D^2)^{m+1} - A^{m+1}}{D^{m+2} * x^m * 22.13^m} \tag{2}$$

where L is the slope length factor for a given raster cell (pixel), A is the upstream catchment area (m^2) at the cell inlet (limited to 10 hectares), D is the raster cell width (m), m is the slope length exponent, $x = \sin a + \cos a$, with α being the slope aspect.

The slope length exponent m is calculated depending on the rill to inter-rill ratio β and the slope gradient θ (Foster et al. 1977 and McCool et al. 1989, cited in Renard et al. 1997):

$$\beta = \frac{\frac{\sin\theta}{0.0896}}{3 * (\sin\theta)^{0.8} + 0.56} \tag{3}$$

$$m = \frac{\beta}{1+\beta} \tag{4}$$

We apply a revised slope factor, S, which is calculated according to a threshold in slope gradient sp (%) (Renard et al. 1997):

$$S = \begin{cases} 10.8 * \sin\theta + 0.03 & with\ sp < 9\% \\ 16.8 * \sin\theta - 0.5 & with\ sp \geq 9\% \end{cases} \tag{5}$$

Furthermore, we apply a revised *K* factor in the NZUSLE developed in Neverman et al. (2021b) to better represent the spatial variability of soil erodibility, utilising the Fundamental Soils Layer (FSL) to represent soil parameters. We adapted the *K* factor equations in Wang et al. (2001) and Yang et al. (2018) to the NZUSLE:

$$K = \frac{2.1(12 - OM)M^{1.14}10^{-4} + 3.25(SS - 2) + 2.5(PP - 3)}{7.59\ x\ 10} \tag{6}$$

where *OM* is the soil organic matter content, *M* is the particle size parameter, *SS* is the soil structure code, and *PP* is the soil profile permeability code. We use 6 *PP* classes, adapted from Rosewell & Loch (2002). The soil structure code was set at *SS* = 2 as the FSL has insufficient data on soil structure to relate to the *SS* classes used for calculating *K*. We found the magnitude of *K* was not sensitive to the choice of *SS* class value. *M* is calculated as a function of the proportion silt and clay:

$$M = Silt(100 - Clay) \tag{7}$$

where *Silt* and *Clay* are the percent of silt and clay in the soil, respectively.

Silt was limited to a range of 15–70%, and *OM* was capped at 4% to fit the nomograph of Wischmeier et al. (1971) used to derive Equation 6 for organic soils.

To incorporate the impact of winter forage cropping on surficial erosion a modified C factor was used in winter forage cropping paddocks (C_{WF}) to represent the temporal variability in cover. Where forage cropping occurs, it is assumed the paddock has an average vegetation cover with a C factor equivalent to pasture for 9 months of the year, and equivalent to bare ground for 3 months of the year as a result of the sowing and grazing cycles. C_{WF} is therefore calculated as:

$$C_{WF} = 0.75C_P + 0.25C_B \tag{8}$$

where C_P is the C factor for pasture and C_B is the C factor for bare ground. This gives a C factor of 0.2575 for winter forage cropping in the NZUSLE.

The location of winter forage cropping paddocks as mapped by Belliss et al. (2019) were incorporated into the landcover layer for the Otago region. This layer is limited to hill-country areas, classified as land with a slope of ≥7° (Belliss et al. 2019).

4.1.2 Bank erosion

SedNetNZ represents bank erosion at the reach-scale where the river network is divided into stream links based on the digital network underpinning the River Environment Classification (REC v2). The total mass of material eroded from riverbanks each year is a function of bank height, reach length, and bank migration rate (Dymond et al. 2016):

$$B_j = \rho M_j H_j L_j \tag{9}$$

where B_j is the total eroded mass for the jth stream link (t y^{-1}), ρ is the bulk density of the bank material (t m^{-3}), M_j is the bank migration rate (m y^{-1}), H_j is the mean bank height (m) and L_j is the length (m) of the jth stream link. Bank height is derived from a relationship with mean annual discharge and bulk density is estimated at 1.5 t m^{-3} (Dymond et al. 2016).

The predicted mass of material eroded from riverbanks represents the gross contribution of sediment supplied to the river channel per year. This does not account for redeposition and storage of eroded bank material on banks, within the channel bed or the lateral accretion of material on bars with channel migration. Hence, net bank erosion in SedNetNZ is estimated as one-fifth of gross bank erosion based on results from the Waipaoa River catchment (De Rose & Basher 2011). Overbank vertical accretion of fine sediment on floodplains beyond the active channel is represented separately (Dymond et al. 2016).

Bank migration rate (M_j) in equation 10 is represented as a function of six factors as follows:

$$M_j = SP_j Sn_j T_j V_j \left(1 - PR_j\right)\left(1 - PW_j\right) \tag{10}$$

where M_j is the bank migration rate (m y^{-1}) of the jth stream link, SP_j is the stream power of the mean annual flood for the jth stream link, Sn_j is the channel sinuosity rate factor of the jth link, T_j is the soil texture-based erodibility factor of the jth link, V_j is the valley confinement factor of the jth link, PR_j is the proportion of riparian woody vegetation of the jth link, and PW_j is the fraction of bank protection works for the jth link (Smith et al. 2019b)

Stream power (SP_j) for the mean annual flood (MAF_j, m^3 s^{-1}) is estimated for each stream link by the product of mean annual flood and channel slope (S_j). MAF is estimated from a fitted power relationship ($MAF = aq^b$) with mean annual discharge (q, m^3 s^{-1}) using data from long-term river flow gauging within the catchment or region of interest:

$$SP_j = MAF_j S_j = a{q_j}^b S_j \quad (11)$$

Various studies report increasing bank migration rates with increasing bankfull discharge and stream power (Hooke 1979; Nanson & Hickin 1986; Walker & Rutherfurd 1999; Alber & Piégay 2017). While MAF has been shown to relate to bank erosion rates (Dymond et al. 2016), other factors, such as channel sinuosity (Nanson & Hickin 1983), the cohesiveness of bank materials (Julian & Torres 2006), valley confinement (Hall et al. 2007), and riparian woody vegetation (Abernethy & Rutherfurd 2000), are also important, resulting in high levels of spatial variability in bank erosion.

We use the log-normal probability density function to represent the relationship between channel sinuosity and migration rate, which we term the sinuosity rate factor. This function allows us to represent the positive-skew observed in the relationship between channel sinuosity and migration rate (Crosato 2009). The dimensionless channel sinuosity rate factor (Sn_j) is calculated as

$$Sn_j = \frac{1}{(Sinu_j - 1)\sigma\sqrt{2\pi}}\, e^{\left(-\frac{\left(\ln(Sinu_j - 1) - \mu\right)^2}{2\sigma^2}\right)} \quad (12)$$

where $Sinu_j$ is sinuosity of the jth stream link of the REC2 network, and μ and σ are the mean and standard deviation parameters that determine the location and scale of the distribution. The μ and σ parameters are fitted using measurements of reach-scale bank migration rates.

The texture of bank material influences bank migration rates (Hickin & Nanson 1984; Julian & Torres 2006; Wynn & Mostaghimi 2006). Our approach is based on an empirical relationship between percent silt + clay content (SC) and soil critical shear stress (τ_c) derived by Julian and Torres (2006) using data from Dunn (1959) as follows:

$$\tau_c = 0.1 + 0.1779SC + 0.0028SC^2 - 0.0000234SC^3 \quad (13)$$

SC is obtained from spatial data on soil textural classes compiled from the Fundamental Soil Layers (FSL) (Newsome et al. 2008), which provide national coverage. The soil texture-based erodibility factor (T_j) is represented by a power function to characterise the relationship between τ_c and bank erodibility for the jth stream link:

$$T_j = c{\tau_{c,j}}^{-d} \quad (14)$$

where the c and d parameters are fitted using available bank migration rate data. The choice of a power function is based on experimental (Arulanandan et al. 1980) and field (Hanson & Simon 2001; Julian & Torres 2006) observations of the relationship between stream bank or bed critical shear stress and erodibility.

Floodplain extent and the level of valley confinement are factors that may limit lateral bank migration (Hall et al. 2007; De Rose & Basher 2011). The presence of steep valley sides and/or exposure of bedrock influence spatial patterns of erosion and deposition (Fryirs et al. 2016). Here, we adapt the Australian SedNet model approach (Hughes & Prosser 2003; Wilkinson et al. 2005) to estimate a valley confinement factor (V_j) by using the mean slope (SB_j) in degrees of a buffer zone either side of the jth stream link:

$$V_j = \left(1 - e^{\left(-15/_{SB_j}\right)}\right)^{11} \tag{15}$$

Woody riparian vegetation typically increases bank stability via the effects of root reinforcement and root cohesion (Abernethy & Rutherfurd 2000; Hubble et al. 2010; Polvi et al. 2014; Konsoer et al. 2016). Woody vegetation can also increase roughness and flow resistance, thereby reducing the boundary shear stress acting on the bank surface (Thorne 1990). In addition, woody vegetation has hydrological effects on bank stability. For example, woody vegetation was found to be more effective than grass cover in lowering soil water content due to increased canopy interception and evapotranspiration, thus improving bank stability (Simon & Collison 2002).

We represent the effect of riparian woody vegetation (PR_j) in reducing bank migration rates at the reach scale. Bank migration rates are reduced proportionally to the extent of woody riparian vegetation along the jth stream link (equation 10). Stream links with complete riparian woody vegetation cover are assumed to erode at 0.05 of the migration rate with no woody cover (De Rose et al. 2003). Spatial information on woody vegetation is obtained from satellite imagery and intersected with the Land Information New Zealand (LINZ) digital stream network obtained from 1:50,000 topographic mapping. The mapped stream network was used in preference to the DEM-derived channel network because it tends to exhibit better planform accuracy which should improve spatial correspondence between channel position and riparian woody vegetation.

In some cases, the LINZ stream network provides poor representation of channel width for wider reaches with exposed gravel. To address this issue, the spatial union of the LINZ river polygons with LCDB v5 'river' and 'gravel and rock' land cover classes was used to produce revised river polygons. Mapped gravel and rock areas located beyond the extent of the channel network were removed. The proportion of riparian woody vegetation is computed from the intersection of the revised stream network with a 15-m buffer and a classified map of 2002 woody vegetation cover (called EcoSat Woody) derived from Landsat TM at 15-m resolution (Dymond & Shepherd 2004).

We also include representation of channel protection works (PW_j) that are designed to reduce bank erosion (e.g. rock riprap, willow edge protection) as well as stopbanks employed for flood protection, where such data are available. We assume that over the multi-decadal model timescale, erosion mitigation would ultimately be targeted to where migrating riverbanks approach stopbanks, or that such interventions have already been implemented to protect stopbank integrity. The proportional length of bank erosion control measures (PEC_j) and stopbanks (PSB_j) is summed to give the proportion of channel works (PW_j) for the jth stream link. PEC_j is computed as the length of erosion control measures within a stream link relative to the total length of that link. This assumes erosion control measures are targeted to the eroding bank side. Stopbanks may be located on either side of the channel irrespective of the direction of bank migration. Therefore, PSB_j is computed as the length of stopbanks in a link relative to 2 × link length.

Inputs to the bank erosion model component of SedNetNZ were obtained from national-scale spatial datasets comprising the REC2 and LINZ stream networks, 15-m DEM, FSL for soil data, and EcoSat Woody for 2002 woody vegetation cover. LCDB v5 was not used, despite being more recent because it has a minimum mapping unit of 10,000 m^2 versus 225 m^2 for EcoSat. This makes LCDB less suitable for characterising narrow corridors of woody vegetation often found along channel banks.

Mean annual discharge estimated for each link in the REC2 stream network is based on an empirical water balance model (Woods et al. 2006) used in the CLUES water quality model (Elliot et al. 2016). Hydrological data provided by ORC comprised mean annual flood statistics for 53 gauging stations with records >10 years in length from across the region. These data were used to fit a relationship (Fig. 1) between mean annual discharge and mean annual flood ($MAF = 44q^{0.5}$, R^2 = 0.80) for use in calculating stream power for each REC2 link in the stream network. ORC also provided spatial data on stopbanks which have been included in the model simulations. However, spatial information on channel erosion control works (e.g., riprap, etc.) was not available.

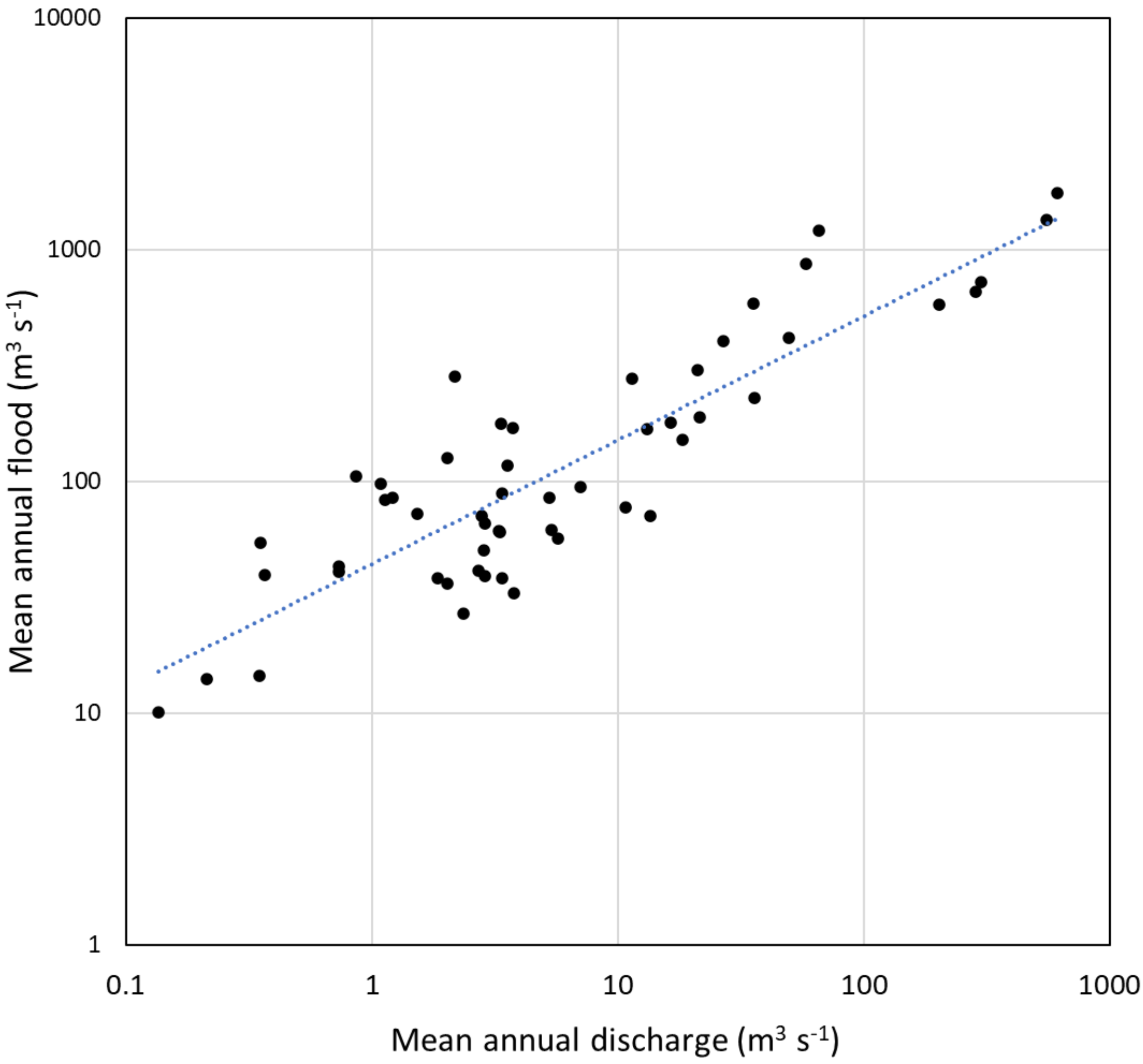

Figure 1. Fitted power relationship between mean annual discharge and mean annual flood (MAF) based on data from river gauging stations across Otago.

In the absence of mapped reach-scale channel changes within the Otago region, we used a combined dataset comprising measured bank migration rates from the Manawatū and Kaipara catchments to calibrate the bank erosion model (Spiekermann et al. 2017; Smith et al. 2019b). This calibration dataset has also been used in other recent applications of SedNetNZ in Hawke's Bay (Smith et al. 2020), Southland (Smith et al. 2019a; Neverman et al. 2021b), Taranaki (Neverman et al. 2021a), and Bay of Plenty (Vale et al. 2021). Calibration of the bank migration model was performed by minimising the mean square error (MSE) between predicted and observed data by optimising parameter values for the sinuosity (μ and σ) and bank soil texture (c and d) factors in equations 12 and 14, respectively. This produced reasonable agreement between measured and observed bank migration rates (Smith et al. 2019b; Fig. 2).

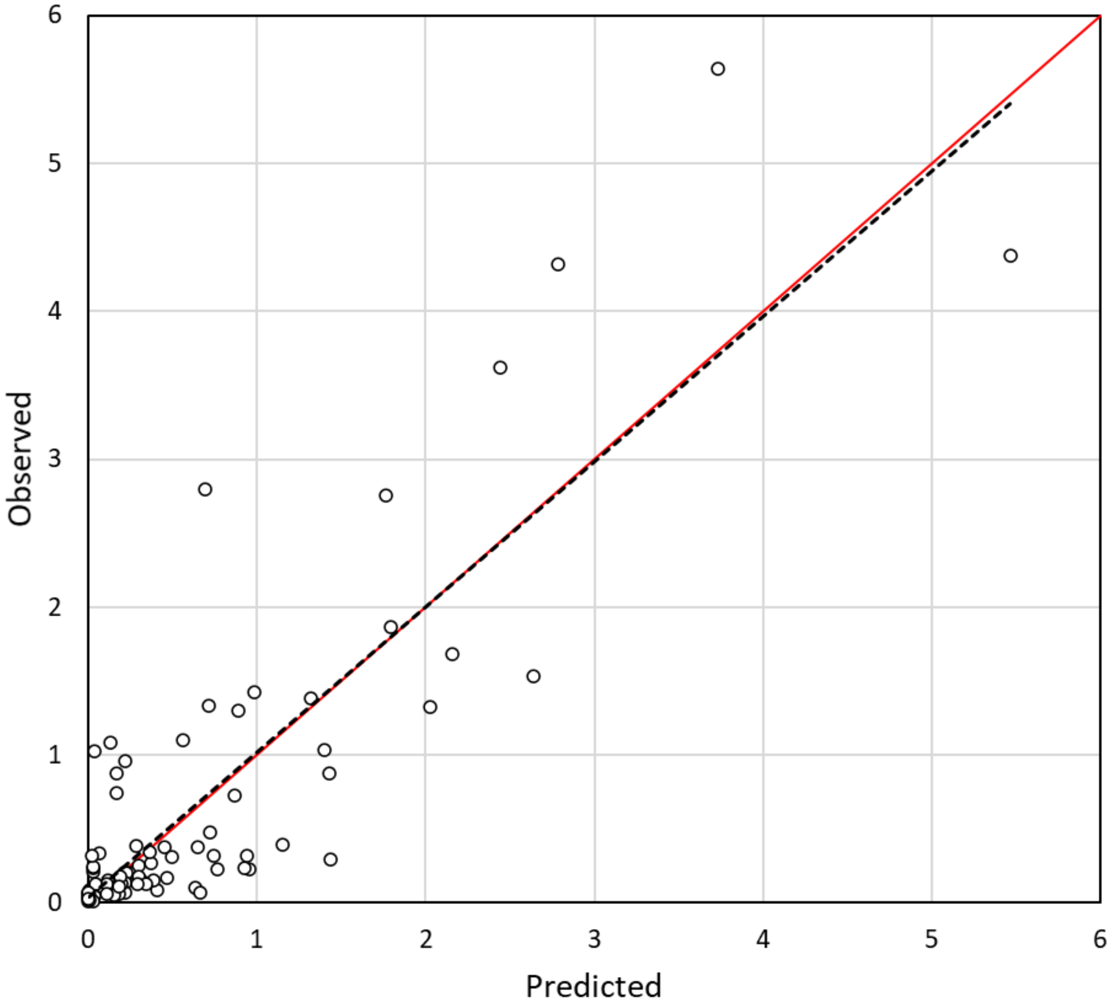

Figure 2. Plot comparing predicted versus observed bank migration rates (m y^{-1}) based on calibrated parameter values for the sinuosity and erodibility factors. Fitted regression line (black dashed) and the 1:1 line (red) are also shown.

4.1.3 Sediment routing

SedNetNZ accounts for the deposition of sediment in lakes and on floodplains as the sediment is transported through the channel network.

To account for sediment trapping in lakes, we apply a revised SedNetNZ sediment routing algorithm. The revised routing algorithm applies a lake-specific sediment passing factor (*SPF*) to the net routed sediment load at the end of a REC2 sub-catchment draining to a lake. *SPF* was calculated using an adaptation of Gill's (1979) approximation of Brune's (1953) trap efficiency (the inverse of passing factor) curve for medium-sized sediment:

$$SPF = 1 - \frac{V/_I}{1.02(V/_I) + 0.012} \quad (16)$$

where V is the lake volume and I is the annual inflow to the lake. This is similar to the approach of Hicks et al. (2019).

The mass of sediment deposited on the floodplain in a given reach is calculated as:

$$F_i = pS_t \frac{L_i accS_i^2}{\sum L_i accS_i^2} \quad (17)$$

where F_i is the total floodplain deposition (t y^{-1}) in the ith sub-catchment, p is the proportion of the sediment load generated by hillslope erosion per lake or sea-draining catchment that is deposited on floodplains in the catchment, set to 5% based on previous SedNetNZ parameterisation carried out in the Manawatū (Dymond et al. 2016), S_t is the total sediment (t y^{-1}) generated by hillslope erosion per lake or sea-draining catchment, L_i is the reach length (m) on floodplain in the ith sub-catchment, and $accS_i$ is the total accumulated (upstream) sediment from hillslope erosion (t y^{-1}) in the ith sub-catchment.

4.2 Selecting monitoring sites for analysis

Baseline visual clarity data for 116 SoE monitoring sites across the Otago region were provided by ORC. The visual clarity baselines at SoE sites were modelled from turbidity measurements using Franklin et al.'s (2019) relationship between turbidity and visual clarity calibrated on a national dataset (ORC, pers. comm., 27 April 2021). Only sites with a contemporary attribute state below an A band, without a dominantly glacial source of flow[1], and with ≥5 years of turbidity data available in 2017 (c.f. interpretation of baseline state in NPS-FM 2020) were included for further analysis. This provided a set of sites with improvable attribute states, and with sufficient baseline data to meet NOF requirements.

During the analysis several sites were found to have been assigned the wrong suspended sediment class (defined according to Hicks et al 2020). Correcting the suspended sediment

[1] Segments whose flow is primarily sourced from glacial segments were identified by Hicks et al. 2019 for the REC2 digital river network, and are provided as a shapefile layer at https://data.mfe.govt.nz/layer/103687-hydrological-modelling-to-support-proposed-sediment-attribute-impact-testing-2020/.

class for all monitoring sites resulted in a change in baseline attribute state for four sites (Table 1).

Table 1. SoE sites with incorrect sediment class in supplied data

Site ID	Initial Sediment Class	Corrected Sediment Class	Initial Attribute State	Corrected Attribute State
Sutton Stream at SH87	1	3	C	D
Taieri at Sutton	1	3	D	D
Tokomairiro at Lisnatunny	2	1	A	D
Waipori at Waipori Falls Reserve	1	3	A	D

Three sites were also found to have been assigned the incorrect attribute state for their respective sediment class and baseline visual clarity (Table 2).

Table 2. SoE sites with correct sediment class but incorrect baseline attribute state

Site ID	Initial Attribute State	Corrected Attribute State
Catlins at Houipapa	D	B
Owaka at Katea Road	D	A
Waipahi at Waipahi	D	A

Following correction of the site attributes, 34 of the 116 SoE sites were found to meet the selection criteria for further analysis (Table 3). 61 sites in total had record lengths of ≥5 years, with 27 sites already achieving band A.

Table 3. SoE sites meeting criteria for inclusion in this analysis, following correction of site attributes

Site ID	Site No.	Suspended sediment class	Contemporary attribute state	Baseline visual clarity (m)
Benger burn at SH8	1	3	D	1.90
Catlins at Houipapa	2	4	B	1.33
Clutha @ Balclutha	3	3	D	1.51
Clutha @ Millers Flat	4	3	D	2.15
Crookston Burn at Kelso Road	5	1	D	1.20
Heriot Burn at Park Hill Road	6	1	D	0.93
Kawarau @ Chards Rd	7	3	C	2.52
Kye Burn at SH85 Bridge	8	3	C	2.35
Lindis at Ardgour Road	9	3	B	2.70
Lindis at Lindis Peak	10	3	C	2.46

Site ID	Site No.	Suspended sediment class	Contemporary attribute state	Baseline visual clarity (m)
Lindsays Creek at North Road Bridge	11	1	C	1.50
Lovells Creek at Station Road	12	1	D	1.14
Manuherikia at Blackstone Hill	13	3	D	2.04
Manuherikia at Galloway	14	3	D	1.69
Manuherikia at Ophir	15	3	D	1.60
Mill Creek at Fish Trap	16	3	D	1.39
Owhiro Stream at Riverside Rd	17	1	D	0.40
Pomahaka at Burkes Ford	18	1	D	1.29
Pomahaka at Glenken	19	3	D	1.76
Sutton Stream at SH87	20	3	D	1.50
Taieri at Allanton Bridge	21	3	D	1.12
Taieri at Creamery Road bridge	22	3	D	1.69
Taieri at Linnburn Runs Road	23	3	C	2.50
Taieri at Outram	24	3	C	2.34
Taieri at Stonehenge	25	3	C	2.50
Taieri at Sutton	26	3	D	1.21
Taieri at Tiroiti	27	3	D	0.73
Taieri at Waipiata	28	3	D	1.52
Thomsons Creek at SH85	29	3	D	1.22
Tokomairiro at Lisnatunny	30	1	D	1.24
Tokomairiro at West Branch Bridge	31	1	B	1.62
Waipori at Waipori Falls Reserve	32	3	D	2.20
Wairuna at Millar Road	33	1	D	0.66
Waitahuna at Tweeds Bridge	34	1	D	1.14

Table 4. Count of SoE sites in each band under the baseline scenario. Sites are only counted in the highest band with which they comply, i.e. if a site is counted in the A band it is not counted in band B, although it would also comply with band B

Attribute Band	Number of sites in attribute band
A	0
B	3
C	7
National bottom line	0
D	24
Total	**34**

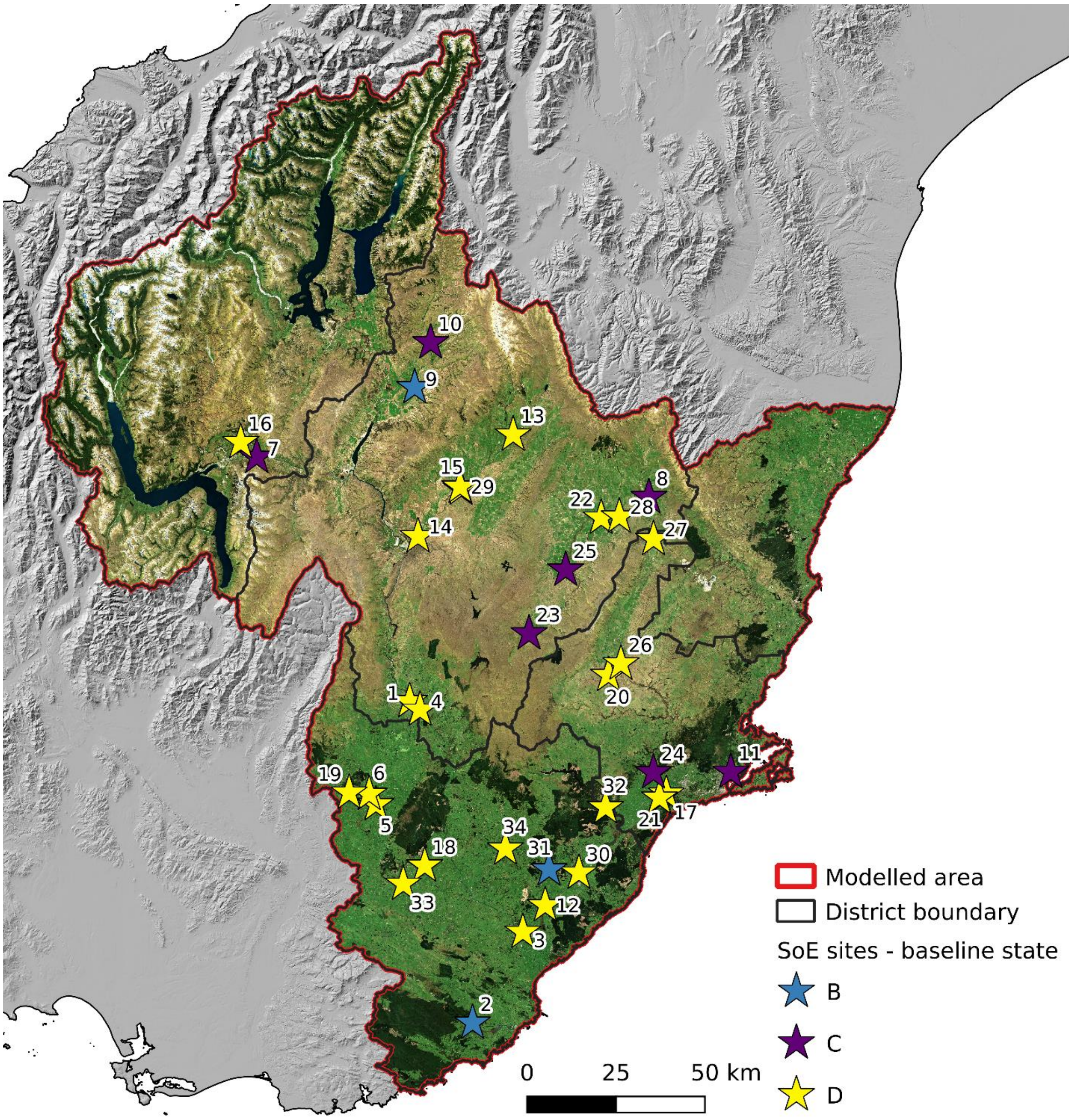

Figure 3. Location of the 34 SoE sites which have a baseline attribute state below band A. See Table 3 for site numbering.

4.3 Application of SedNetNZ to Otago

Modelling suspended sediment loads at the 34 SoE sites selected for analysis requires computation of erosion yields in all REC2 watersheds upstream of each SoE site, and the downstream accumulation of individual watershed suspended sediment loads to each SoE site, while accounting for lake and floodplain deposition. The area modelled for this report (Fig. 3) therefore comprises all REC2 watersheds draining to the 34 SoE sites selected for analysis, as well as continuation of the river networks to the coast.

In applying SedNetNZ to the Otago region, we consider suspended sediment loads to be primarily driven by surficial and bank erosion. We acknowledge a complex array of erosion processes occur in the mountainous headwaters that are not explicitly represented by SedNetNZ. However, these processes primarily deliver coarse sediment to the channel network which does not contribute to suspended sediment loads. Only a small fraction of suspended sediment from mountainous headwaters in the Southern Alps contributes to suspended sediment loads at the 34 SoE sites analysed in this report due to the interception of suspended sediment by the major lakes, which trap ≥97% of suspended sediment loads and are situated upstream of the SoE sites in their respective catchments.

4.4 Model simulations

SedNetNZ model simulations were completed for two scenarios. The first scenario represents land cover for the nominal baseline year of 2017, which is the year used to calculate baseline visual clarity. This scenario uses the 2018 land cover from LCDB, the extent of winter forage cropping as mapped by Belliss et al (2019), and an estimate of the contemporary extent of riparian fencing in each district based on the 2017 Survey of Rural Decision Makers (Stahlmann-Brown 2021). A second scenario is modelled using the same land cover information as for the baseline in combination with an aspirational extent of riparian fencing, which involved fully fenced streams on all land deemed mitigatable. The aspirational scenario aims to represent an ambitious upper limit in sediment load reductions that may be achievable with a maximal extent of riparian fencing. The sediment loads produced by SedNetNZ for each scenario represent the multidecadal annual average suspended sediment loads expected if the land cover and spatial extent of riparian fencing were held constant.

Table 5. Summary of land cover scenario configurations

Baseline scenario	• New Zealand Landcover Database (LCDB) version 5 is used to represent land cover, with inclusion of winter forage crop extent from Belliss et al. (2019). • Segments <3rd order in the REC network were classified as minor streams, and segments ≥3rd order were classified as major streams. • The length of stream segments adjacent to low and high producing pasture, cropland, orchards, vineyards, or perennial crops, as classified by LCDB v5 2018, was deemed suitable for mitigation (application of riparian fencing). • Riparian fencing with a 3 m buffer was applied to the portion of the mitigatable length of each major and minor stream segment equivalent to the proportion of major and minor streams fenced in each region according to the SRDM (Table 6).
Aspirational scenario	• Same land cover configuration as used in the baseline scenario. • 100% of the mitigatable length of each stream segment was fenced with a 3-m buffer.

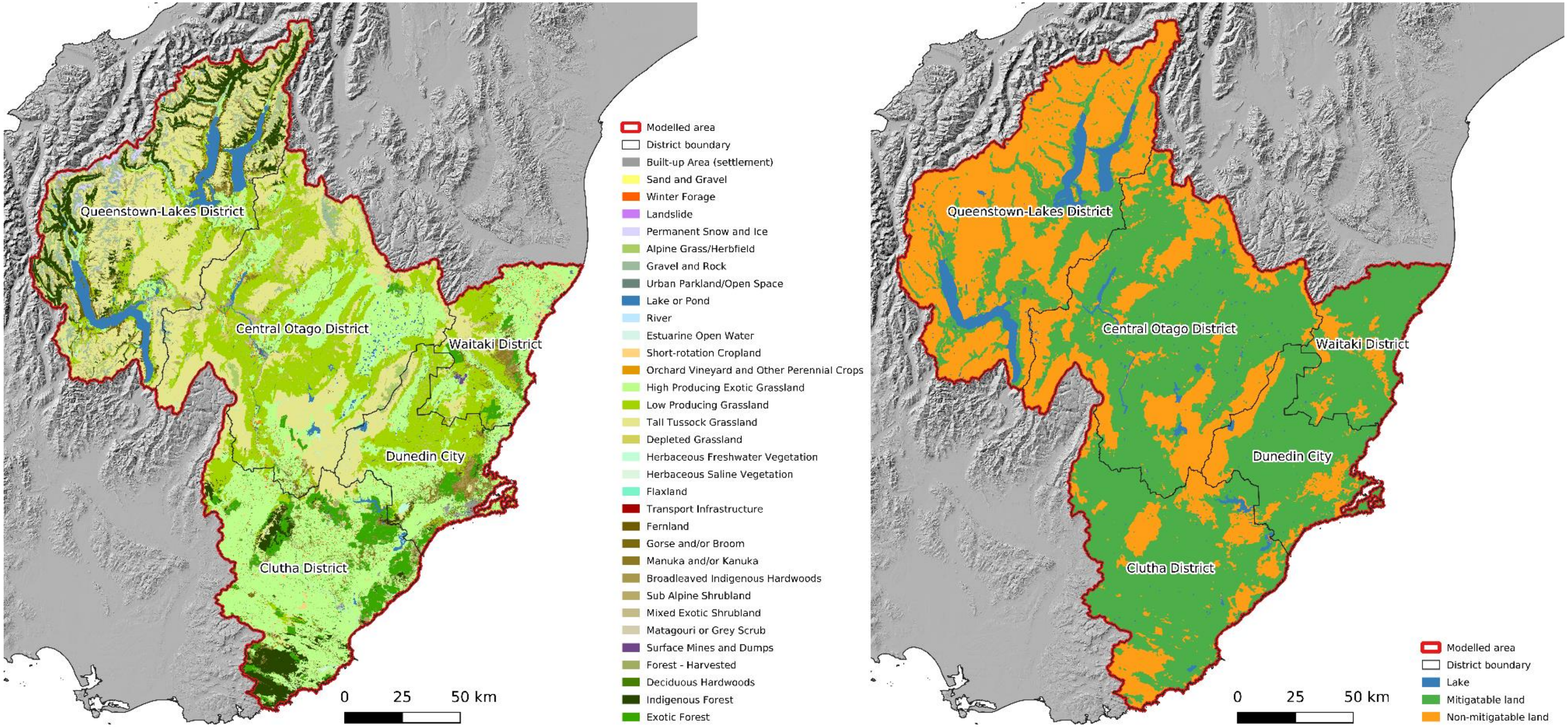

Figure 4. Land cover as represented by LCDB 2018 with the inclusion of winter forage cropping (left) and areas classified as mitigatable vs non-mitigatable land (right).

4.4.1 Riparian fencing

Riparian fencing was applied to the proportion of all stream segments intersecting low and high producing pasture, cropland, orchards, vineyards, and perennial crops, as classified by LCDB version 5 for 2018 (Fig. 4). Riparian fencing is represented spatially in the model using an estimate of implemented fencing by district for major and minor streams (Fig. 5) based on results from the 2017 Survey of Rural Decision Makers (SRDM, Stahlmann-Brown 2021) (Table 6) following Neverman et al. (2019) and Monaghan et al. (2021). Minor streams are classified as segments <3rd order in the REC network, and major streams as segments ≥3rd order.

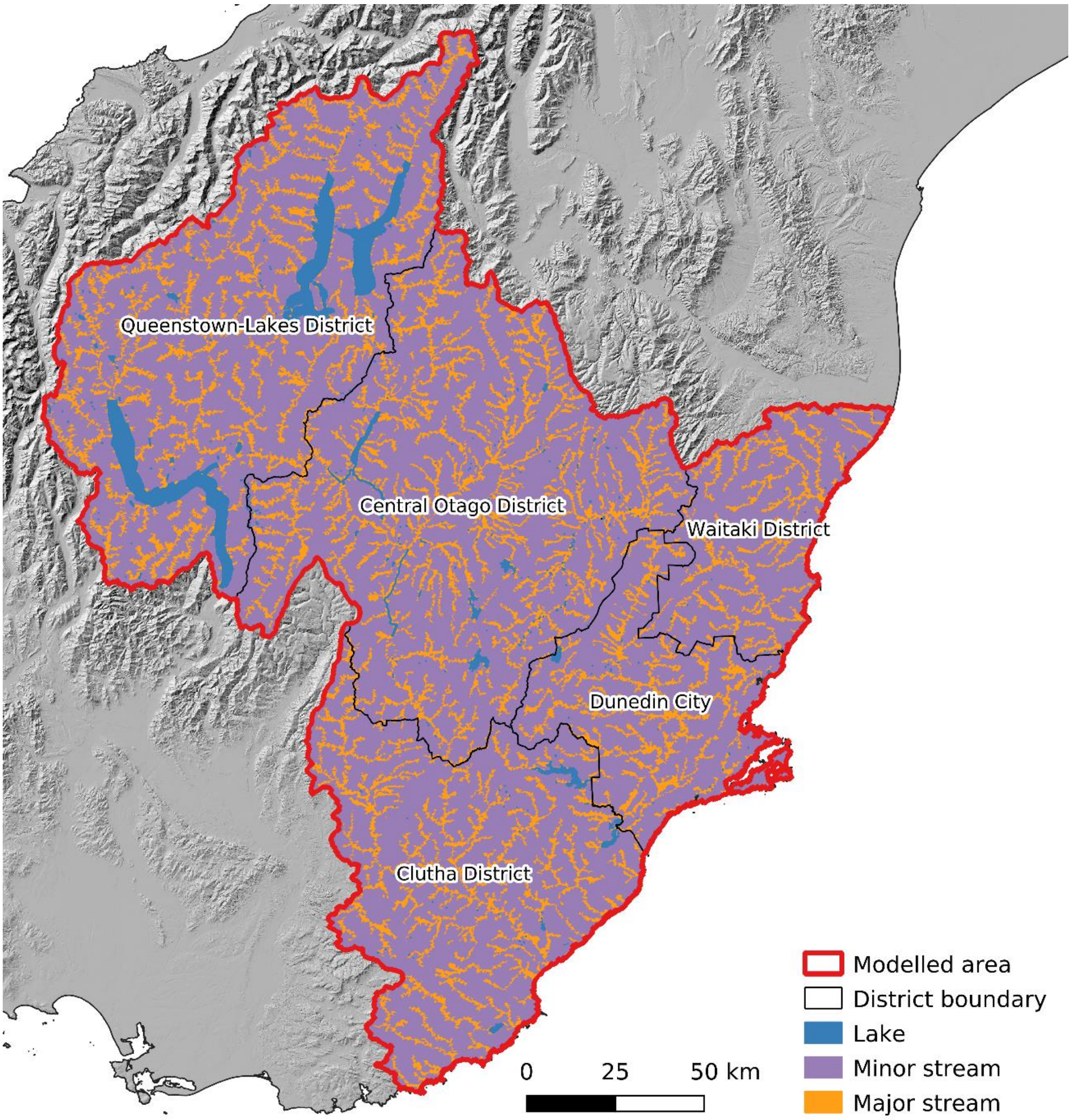

Figure 5. Distribution of minor and major stream segments.

Table 6. Proportion of major and minor streams estimated to be fenced based on the Survey of Rural Decision Makers 2017

District	Minor streams fenced 2017 (%)	Major streams fenced 2017 (%)
Central Otago	19.7	18.8
Clutha	46.1	40.1
Dunedin City	34.4	35.4
Queenstown-Lakes[2]	0	0
Waitaki	57.9	39.6

[2]. While it is likely some fencing has been implemented in the Queenstown-Lakes District to date, we were unable to derive an estimated extent due to a low number of respondents to the SRDM from the Queenstown-Lakes District. We have therefore used a baseline value of zero that allows the maximum level of fencing to be implemented between the baseline and aspirational states.

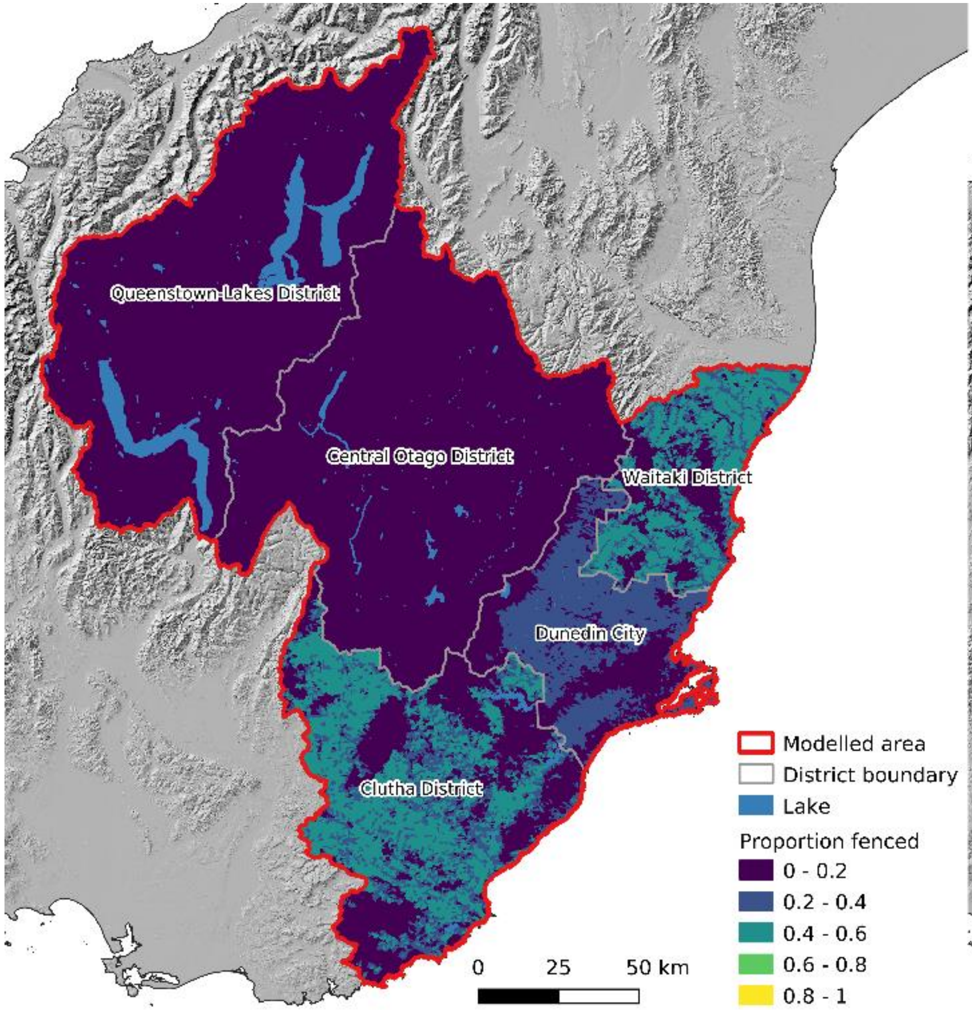

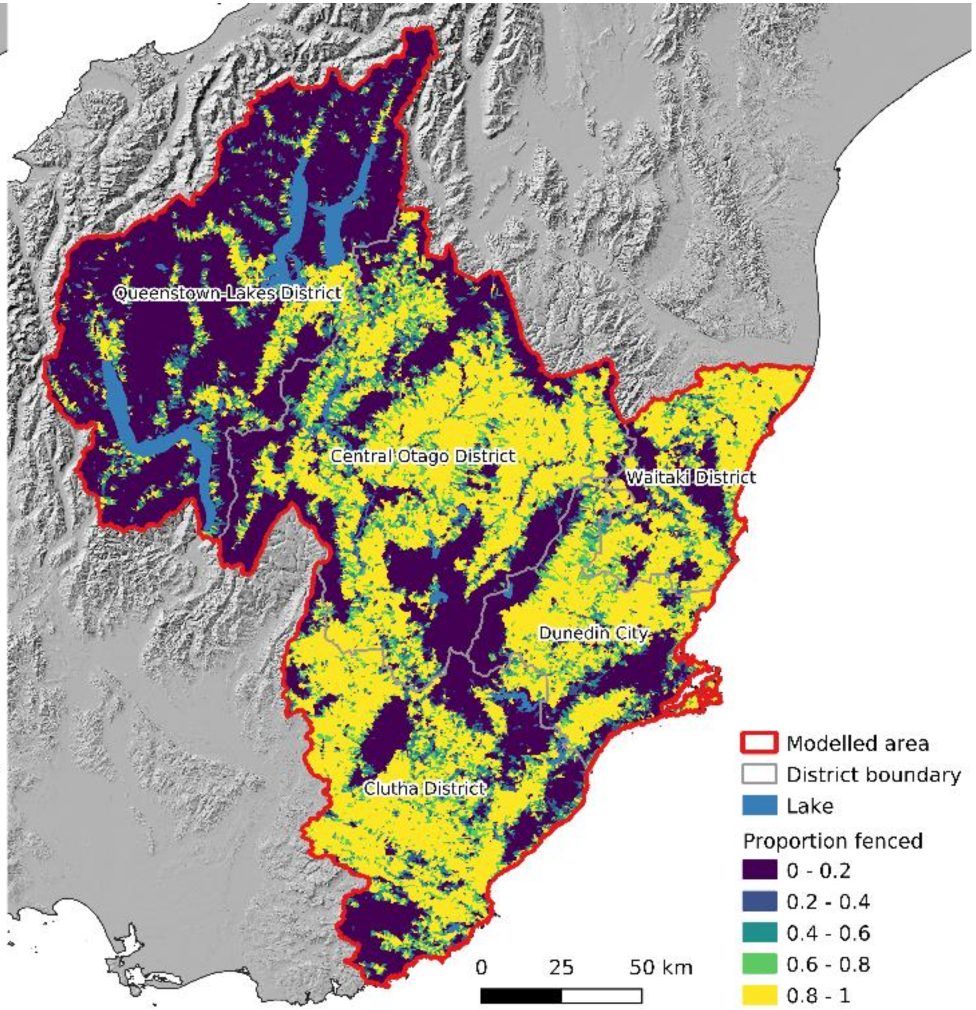

Figure 6. Proportion of stream segment fenced in baseline scenario (left) and aspirational scenario (right).

To identify the proportion of a stream segment suitable for application of riparian fencing we applied a 60-m buffer to the REC2 digital stream network and used this to identify land cover along each stream segment. This buffer is designed to accommodate variations in channel width as well as positional error evident in REC2 stream segments relative to channel banks and adjoining land cover. Low and high producing pasture, cropland, orchards, vineyards, or perennial crops within LCDB were deemed to be suitable for application of riparian fencing, and are defined as *mitigatable land*. The length of stream segment intersecting mitigatable land was summed per REC2 stream link and used in determining the effect of fencing on bank erosion for each segment.

The reduced net suspended sediment load from bank erosion due to fencing and stock exclusion (B_{F_j}) is computed as:

$$B_{F_j} = B_j \times (1 - 0.8FR_j) \tag{18}$$

where B_j is the net suspended sediment load from bank erosion without the effect of fences reducing erosion, and FR_j is the proportion of segment with riparian fencing. A reduction of 80% in net suspended sediment load from bank erosion may be attributable to riparian fencing and stock exclusion (Dymond et al. 2016). This reflects the effect of reduced stock trampling and foraging on banks (Trimble 1994) as well as the potential for riparian woody vegetation to become better established in the absence of livestock over the longer-term.

The inclusion of a 3 m vegetated buffer either side of fenced stream channels also reduces surficial erosion loads by intercepting overland flow. This effect is captured in SedNetNZ via a sediment passing factor, the inverse of trapping efficiency. The sediment passing factor is calculated for the buffer for the j-th segment (PF_{Fj}) following Zhang et al. (2010):

$$PF_{F_j} = \frac{1 - k(1 - e^{-bw})}{100} \tag{19}$$

where k and b are fitted parameters, and equal 90.9 and 0.446 (Zhang et al. 2010), respectively. w is the buffer width, modelled as 3 m for all fencing in the region.

The reduction in suspended sediment load from surficial erosion due to the fencing and stock exclusion in a reach (S_{F_j}) is a function of the proportion of reach fenced and the buffer passing factor:

$$S_{F_j} = ES_j \times (1 - FR_j PF_{Fj}) \tag{20}$$

where ES_j is the load from surficial erosion for the j-th reach.

4.5 Future attribute states

The relationships between reductions in mean annual suspended sediment load and increases in median visual clarity developed by Dymond et al. (2017) and subsequently applied by Hicks et al. (2019) nationally were used to calculate the reductions in mean annual suspended sediment loads required to achieve the NOF attribute bands for suspended fine sediment at each SoE monitoring site. The proportional reduction in load required to achieve each attribute band is calculated as a function of the difference between the baseline and minimum numeric attribute state for each band:

$$PR_v = 1 - (V_o/V_b)^{1/a} \tag{21}$$

where PR_v is the minimum proportional reduction in load required to achieve the attribute state, V_o is the minimum visual clarity for each band, and V_b is the baseline median visual clarity. a was assumed to take the national average reported by Hicks et al. (2019) as –0.76.

Given the national bottom line threshold overlaps with the bottom of the range for band C, our analysis looks at reductions required to meet the national bottom line, band B, and band A. Achieving band C requires only a marginal increase in load reduction from that required to achieve the national bottom line.

To identify which attribute band an SoE monitoring site would comply with after aspirational riparian fencing is completed, the reduction in mean annual suspended sediment load between the baseline and aspirational scenarios was compared to the required load reduction to achieve each attribute band. Where the achieved reduction was higher than the required load reduction, the associated attribute band is considered achievable.

Under the NPS-FM 2020, the suspended fine sediment attribute band for a river segment is determined by the median visual clarity at the site, with the threshold visual clarity for each band being determined by the sediment class[3] (see Hicks et al 2020) of the segment (Table 7).

[3] Suspended sediment classes for the REC2 network are available at https://data.mfe.govt.nz/layer/103687-hydrological-modelling-to-support-proposed-sediment-attribute-impact-testing-2020/

Table 7. Attribute bands and numeric attribute states for fine suspended sediment. Reproduced from Table 8 in the NPS-FM 2020

Attribute band and description	Numeric attribute state by suspended sediment class (visual clarity(m))			
	1	2	3	4
A Minimal impact of suspended sediment on instream biota. Ecological communities are similar to those observed in natural reference conditions.	≥1.78	≥0.93	≥2.95	≥1.38
B Low to moderate impact of suspended sediment on instream biota. Abundance of sensitive fish species may be reduced.	<1.78 and ≥1.55	<0.93 and ≥0.76	<2.95 and ≥2.57	<1.38 and ≥1.17
C Moderate to high impact of suspended sediment on instream biota. Sensitive fish species may be lost.	<1.55 and >1.34	<0.76 and >0.61	<2.57 and >2.22	<1.17 and >0.98
National bottom line	1.34	0.61	2.22	0.98
D High impact of suspended sediment on instream biota. Ecological communities are significantly altered, and sensitive fish and macroinvertebrate species are lost or at high risk of being lost.	<1.34	<0.61	<2.22	<0.98

5 Results

5.1 Sediment loads

Under the baseline scenario, 489 kt yr^{-1} of suspended fine sediment are estimated to reach coastal receiving environments in Otago. A 28% reduction in end-of-catchment loads is achieved across the region between the baseline and aspirational scenarios, with 351 kt yr^{-1} of suspended sediment modelled to reach coastal receiving environments with implementation of aspirational mitigations. Suspended sediment loads at the SoE sites are presented in Table 8.

To visualise the distribution of erosion rates, net specific sediment yield (t km^2 yr^{-1}) by REC2 sub-catchment across the region is presented in Figure 7 for each scenario. Net suspended sediment loads are presented in Figure 8.

Table 8. Total mean annual suspended sediment loads at water quality monitoring sites under each modelled scenario, rounded to 2 s.f.

Site ID	Site No.	Baseline suspended sediment load (kt yr^{-1})	Aspirational suspended sediment load (kt yr^{-1})	Load reduction achievable (%)
Benger burn at SH8	1	3.9	1.8	55
Catlins at Houipapa	2	5.1	4.3	17
Clutha @ Balclutha	3	270	200	28
Clutha @ Millers Flat	4	140	120	18
Crookston Burn at Kelso Road	5	1.8	1.3	30
Heriot Burn at Park Hill Road	6	2.8	1.6	45
Kawarau @ Chards Rd	7	410	380	6
Kye Burn at SH85 Bridge	8	23	19	20
Lindis at Ardgour Road	9	59	47	20
Lindis at Lindis Peak	10	47	40	14
Lindsays Creek at North Road Bridge	11	0.4	0.35	11
Lovells Creek at Station Road	12	0.72	0.51	30
Manuherikia at Blackstone Hill	13	13	8.6	32
Manuherikia at Galloway	14	130	110	18
Manuherikia at Ophir	15	120	100	16
Mill Creek at Fish Trap[4]	16	0.042	0.03	27
Owhiro Stream at Riverside Rd	17	0.31	0.18	42
Pomahaka at Burkes Ford	18	56	35	38
Pomahaka at Glenken	19	31	22	30
Sutton Stream at SH87	20	1.9	1.3	33
Taieri at Allanton Bridge	21	110	74	31
Taieri at Creamery Road bridge	22	18	13	26
Taieri at Linnburn Runs Road	23	5.7	5.4	6
Taieri at Outram	24	100	71	31
Taieri at Stonehenge	25	7.5	6.4	14
Taieri at Sutton	26	75	53	29
Taieri at Tiroiti	27	57	42	26
Taieri at Waipiata	28	25	18	28
Thomsons Creek at SH85	29	8.6	6.3	27
Tokomairiro at Lisnatunny	30	0.91	0.76	16
Tokomairiro at West Branch Bridge	31	1.6	1.3	18
Waipori at Waipori Falls Reserve	32	0.85	0.84	1
Wairuna at Millar Road	33	0.64	0.25	61
Waitahuna at Tweeds Bridge	34	6	3.7	38

[4] Mill Creek at Fish Trap is located in a REC2 watershed that contains a lake and therefore has a sediment passing factor applied, hence the smaller load than the immediate upstream segments. This does not affect the outcome of subsequent analysis in this report as the same proportional reduction in load is achieved with or without the sediment passing factor, and therefore the same outcome in visual clarity reduction under the aspirational scenario is achieved.

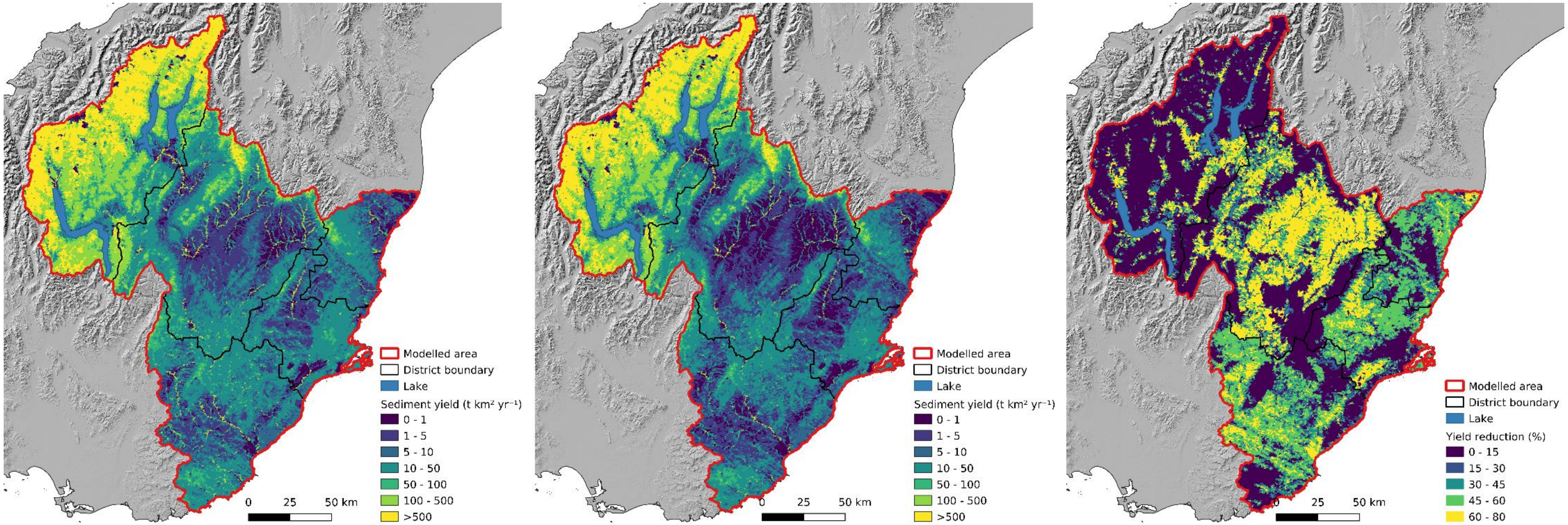

Figure 7. REC2 sub-catchment net suspended sediment yield (t km^2 yr^{-1}) for the baseline (left) and aspirational (centre) scenarios, and the percentage reduction in yield between the scenarios (right).

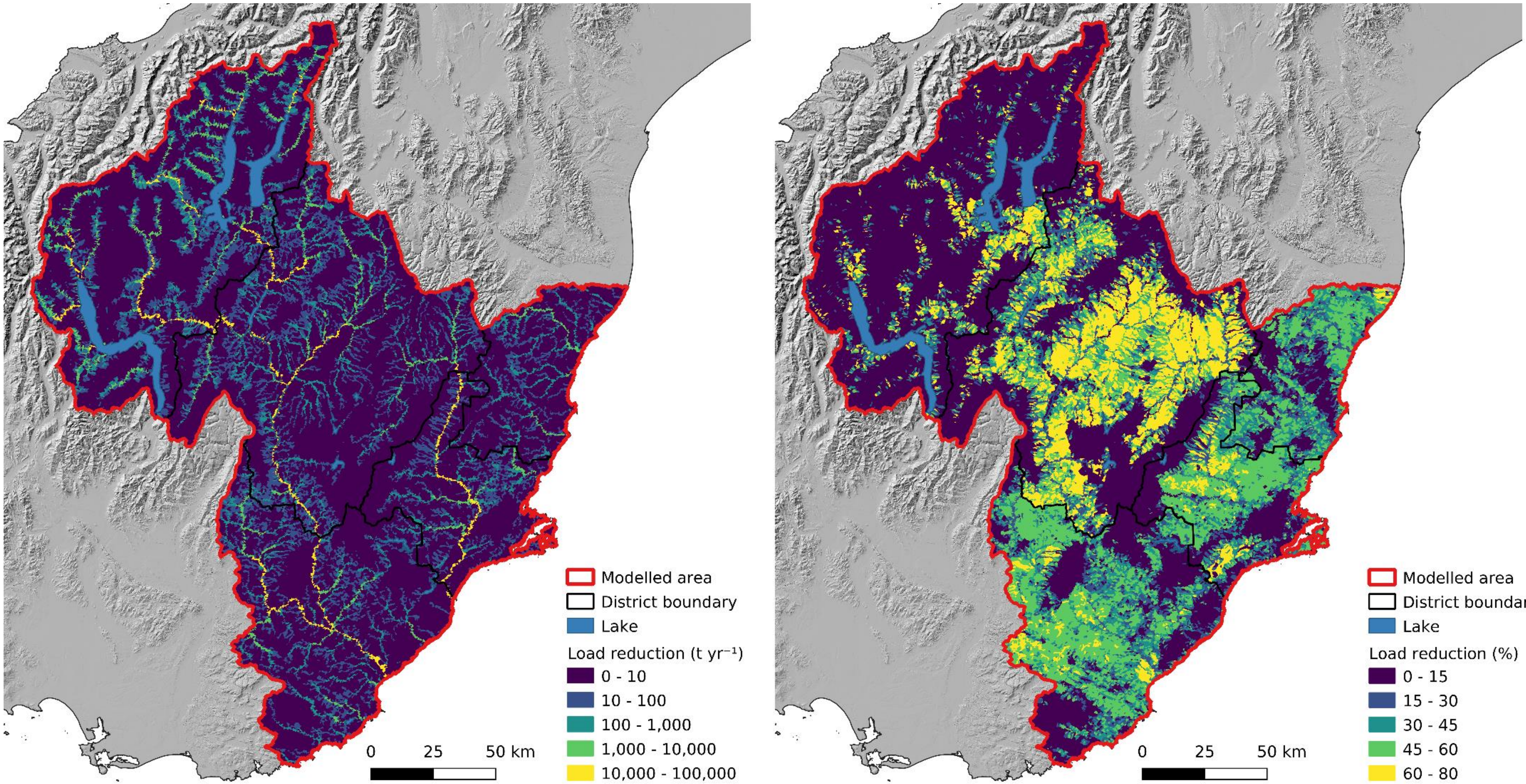

Figure 8. Absolute (left) and proportional (right) REC2 sub-catchment suspended sediment load reductions between the baseline and aspirational scenarios.

5.2 Achievement of NOF attribute states

The proportional and absolute reductions in load required for SoE monitoring sites to achieve each attribute band are presented in Table 9. Where the reduction is zero, the band is already achieved.

Reductions are seen at all 34 analysed SoE sites between the baseline and aspirational scenarios (Table 10). With these reductions six of the 34 SoE sites achieve band A (18%), nine achieve band B (26%), and seven achieve band C (21%) (Table 11). In total, 12 of the 24 (50%) SoE sites with a baseline attribute state in the D band are brought above the national bottom line under the aspirational scenario. 12 of the 34 sites fail to achieve the national bottom line (35%). A comparison of the attribute state for each SoE monitoring site between the baseline and aspirational scenario is presented in Table 12.

Table 9. Proportional and absolute reductions in mean annual suspended sediment load required to achieve NPS-FM 2020 attribute states at water quality monitoring sites, rounded to 2 s.f.

Site ID	Proportional reduction in load required (%)			Absolute reduction in load required (kt yr^{-1})		
	National bottom line	B band	A band	National bottom line	B band	A band
Benger burn at SH8	18	33	44	0.73	1.3	1.7
Catlins at Houipapa	0	0	4	0	0	0.23
Clutha @ Balclutha	40	51	59	110	140	160
Clutha @ Millers Flat	4	21	34	6.4	31	50
Crookston Burn at Kelso Road	13	28	40	0.24	0.52	0.74
Heriot Burn at Park Hill Road	38	49	57	1.1	1.4	1.6
Kawarau @ Chards Rd	0	2	19	0	9.9	76
Kye Burn at SH85 Bridge	0	11	26	0	2.5	6
Lindis at Ardgour Road	0	0	11	0	0	6.4
Lindis at Lindis Peak	0	5	21	0	2.5	9.8
Lindsays Creek at North Road Bridge	0	4	20	0	0.016	0.079
Lovells Creek at Station Road	19	33	44	0.13	0.24	0.32
Manuherikia at Blackstone Hill	11	26	39	1.4	3.4	4.9
Manuherikia at Galloway	30	43	52	40	56	69
Manuherikia at Ophir	35	46	55	42	56	67
Mill Creek at Fish Trap	46	55	63	0.019	0.023	0.026
Owhiro Stream at Riverside Rd	79	83	86	0.25	0.26	0.26
Pomahaka at Burkes Ford	4	21	34	2.5	12	19
Pomahaka at Glenken	26	39	49	8.2	12	15
Sutton Stream at SH87	40	51	59	0.76	0.95	1.1
Taieri at Allanton Bridge	59	67	72	63	71	77
Taieri at Creamery Road bridge	30	43	52	5.4	7.6	9.3
Taieri at Linnburn Runs Road	0	3	19	0	0.19	1.1
Taieri at Outram	0	12	26	0	12	27
Taieri at Stonehenge	0	3	19	0	0.25	1.5
Taieri at Sutton	55	63	69	41	47	51
Taieri at Tiroiti	77	81	84	44	46	48
Taieri at Waipiata	39	50	58	9.8	12	15
Thomsons Creek at SH85	54	62	69	4.7	5.4	5.9
Tokomairiro at Lisnatunny	10	26	38	0.092	0.23	0.35
Tokomairiro at West Branch Bridge	0	0	12	0	0	0.19
Waipori at Waipori Falls Reserve	1	19	32	0.012	0.16	0.27
Wairuna at Millar Road	61	68	73	0.39	0.43	0.47
Waitahuna at Tweeds Bridge	19	33	44	1.1	2	2.7

Table 10. Absolute and proportional reductions in mean annual suspended sediment load under the aspirational scenario relative to baseline at SoE monitoring sites, rounded to 2 s.f.

Site ID	Load reduction achievable (kt yr^1)	Load reduction achievable (%)	Achievable attribute state
Benger burn at SH8	2.2	55	A
Catlins at Houipapa	0.87	17	A
Clutha @ Balclutha	77	28	D
Clutha @ Millers Flat	27	18	C
Crookston Burn at Kelso Road	0.56	30	B
Heriot Burn at Park Hill Road	1.3	45	C
Kawarau @ Chards Rd	23	6	B
Kye Burn at SH85 Bridge	4.6	20	B
Lindis at Ardgour Road	12	20	A
Lindis at Lindis Peak	6.7	14	B
Lindsays Creek at North Road Bridge	0.042	11	B
Lovells Creek at Station Road	0.21	30	C
Manuherikia at Blackstone Hill	4.1	32	B
Manuherikia at Galloway	23	18	D
Manuherikia at Ophir	19	16	D
Mill Creek at Fish Trap	0.011	27	D
Owhiro Stream at Riverside Rd	0.13	42	D
Pomahaka at Burkes Ford	21	38	A
Pomahaka at Glenken	9.5	30	C
Sutton Stream at SH87	0.62	33	D
Taieri at Allanton Bridge	33	31	D
Taieri at Creamery Road bridge	4.6	26	D
Taieri at Linnburn Runs Road	0.37	6	B
Taieri at Outram	31	31	A
Taieri at Stonehenge	1.1	14	B
Taieri at Sutton	22	29	D
Taieri at Tiroiti	15	26	D
Taieri at Waipiata	7	28	D
Thomsons Creek at SH85	2.3	27	D
Tokomairiro at Lisnatunny	0.15	16	C
Tokomairiro at West Branch Bridge	0.3	18	A
Waipori at Waipori Falls Reserve	0.013	1	C
Wairuna at Millar Road	0.4	61	C
Waitahuna at Tweeds Bridge	2.3	38	B

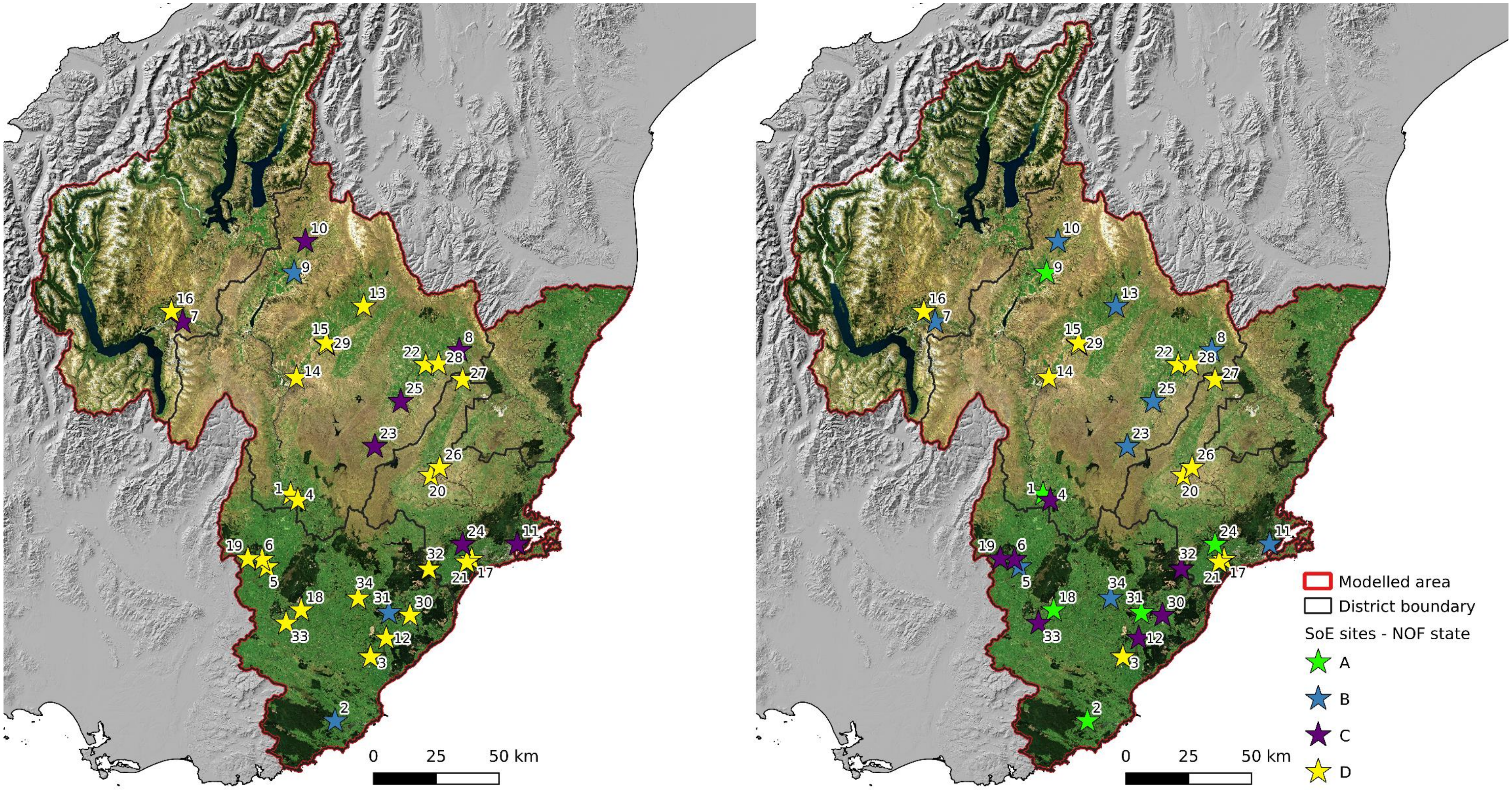

Figure 9. Attribute state achieved under the baseline (left) and aspirational (right) scenarios at the 34 SoE sites.

Table 11. Count of SoE sites in each band under the baseline and aspirational scenarios. Sites are only counted in the highest band with which they comply, i.e. if a site is counted in the A band it is not counted in band B, although it would also comply with the B band

NOF Band	Count of sites achieving band Baseline Scenario	 Aspirational Scenario
A	0	6
B	3	9
C	7	7
National bottom line	0	0
D	24	12
Total	**34**	**34**

Table 12. Comparison of load reductions required to achieve the national bottom line and the reductions achieved in the aspirational scenario at the 12 sites that are unable to achieve the national bottom line

Site ID	Site No.	Suspended sediment class	Baseline visual clarity (m)	National bottom line visual clarity threshold (m)	Reduction required to achieve national bottom line (%)	Load reduction achievable (%)
Clutha @ Balclutha	3	3	1.51	2.22	40	28
Manuherikia at Galloway	14	3	1.69	2.22	30	18
Manuherikia at Ophir	15	3	1.60	2.22	35	16
Mill Creek at Fish Trap	16	3	1.39	2.22	46	27
Owhiro Stream at Riverside Rd	17	1	0.40	1.34	79	42
Sutton Stream at SH87	20	3	1.50	2.22	40	33
Taieri at Allanton Bridge	21	3	1.12	2.22	59	31
Taieri at Creamery Road bridge	22	3	1.69	2.22	30	26
Taieri at Sutton	26	3	1.21	2.22	55	29
Taieri at Tiroiti	27	3	0.73	2.22	77	26
Taieri at Waipiata	28	3	1.52	2.22	39	28
Thomsons Creek at SH85	29	3	1.22	2.22	54	27

Table 13. Comparison of attribute state between the baseline and aspirational scenario at each SoE monitoring site

Site ID	Baseline Band	Aspirational Band
Benger burn at SH8	D	A
Catlins at Houipapa	B	A
Clutha @ Balclutha	D	D
Clutha @ Millers Flat	D	C
Crookston Burn at Kelso Road	D	B
Heriot Burn at Park Hill Road	D	C
Kawarau @ Chards Rd	C	B
Kye Burn at SH85 Bridge	C	B
Lindis at Ardgour Road	B	A
Lindis at Lindis Peak	C	B
Lindsays Creek at North Road Bridge	C	B
Lovells Creek at Station Road	D	C
Manuherikia at Blackstone Hill	D	B
Manuherikia at Galloway	D	D
Manuherikia at Ophir	D	D
Mill Creek at Fish Trap	D	D
Owhiro Stream at Riverside Rd	D	D
Pomahaka at Burkes Ford	D	A
Pomahaka at Glenken	D	C
Sutton Stream at SH87	D	D
Taieri at Allanton Bridge	D	D
Taieri at Creamery Road bridge	D	D
Taieri at Linnburn Runs Road	C	B
Taieri at Outram	C	A
Taieri at Stonehenge	C	B
Taieri at Sutton	D	D
Taieri at Tiroiti	D	D
Taieri at Waipiata	D	D
Thomsons Creek at SH85	D	D
Tokomairiro at Lisnatunny	D	C
Tokomairiro at West Branch Bridge	B	A
Waipori at Waipori Falls Reserve	D	C
Wairuna at Millar Road	D	C
Waitahuna at Tweeds Bridge	D	B

6 Discussion

6.1 Effectiveness of aspirational mitigations

The aspirational mitigations resulted in a 28% reduction in total suspended sediment load reaching coastal receiving environments in the Otago region, equating to a 138 kt yr^{-1} reduction. Due to the trapping effect of the many lakes in the region this may not reflect the total reduction achieved across the region, and likely reflects the impacts of mitigations primarily below the large lakes.

The greatest number of segments achieving high proportional reductions in sediment yield and load are seen in the Central Otago District (Figs 7 and 8), while the fewest segments with reductions occur in the Queenstown-Lakes District. This extent and magnitude of reductions is dependent on a) the extent of fencing estimated to have been implemented by 2017 (Fig. 7), and b) the extent of stream segments determined to be suitable for mitigation (Fig. 4). The combination of these two factors determines the difference in sediment reaching the channel network between the two scenarios in each district. In some districts, such as Clutha and Waitaki, a high proportion of stream fencing is estimated to have been implemented by 2017. As a result, these districts have less capacity for further fencing to be implemented under the aspirational scenario. In the Queenstown-Lakes District no fencing was estimated to have been implemented in 2017, but the district has a relatively small extent of mitigatable land, and as a result shows the smallest areal extent of load reductions (Figs 7 and 8) despite the greatest change in fencing proportionally between the two scenarios.

These relatively high proportional reductions in sediment yield did not necessarily propagate to high load reductions at SoE sites. This is predominantly a result of mitigatable land being located in lowland terrain where surficial erosion rates are relatively low compared to the unmitigatable headwaters, where steeper slopes and higher rainfall drive high erosion rates, often 1–2 orders of magnitude higher than in the lowlands (Fig. 7). As a result, fencing implemented in the aspirational scenario may have a high impact locally, but has a lower impact on accumulated loads, particularly in catchments with high proportions of their load sourced from unmitigatable headwaters (such as in the Queenstown-Lakes and Central Otago Districts). It is therefore important to consider the dominant sources of sediment in catchments when developing mitigation policy and setting objectives for SoE sites.

The impact of mitigations and headwater erosion sources on downstream SoE sites is further complicated in the Otago region by the interception of suspended sediment in lakes. Major lakes such as Lake Wakatipu, Lake Wanaka, and Lake Hawea are modelled to trap ≥97% of instream sediment loads. As a result, the impact of mitigations implemented upstream of major lakes may not be evident at SoE sites downstream of the lakes.

6.2 Improving NOF attribute state

Of the 61 SoE sites with ≥5 years of visual clarity data in 2017, 27 sites (44%) already achieve band A for suspended fine sediment and therefore cannot improve their attribute band, while three sites achieve band B (5%) and seven achieve band C (11%). Of the SoE sites with ≥5 years of visual clarity data, 60% therefore comply with the national bottom line under the NPS-FM 2020 and do not require further improvement. 24 sites (40%) are below the national bottom line and do require a reduction in suspended fine sediment load to comply with the NPS-FM 2020.

Under the modelled aspirational mitigation scenario, a further six sites achieve both band A and band B. In total, 49 sites (80%) comply with the national bottom line under the modelled aspirational mitigation scenario. Of the 61 SoE sites, 20% are therefore brought above the national bottom line for suspended fine sediment.

The 12 sites which remain in band D under the modelled aspirational mitigation scenario belong to either the Clutha or Taieri catchments. The majority of non-compliant sites in the Clutha catchment are located in the Manuherikia catchment, a tributary of the Clutha. The non-compliant sites are often consecutive sites along the tributaries and main stem. Figure 10 demonstrates the nested continuity of non-compliant sites in the Manuherikia and Taieri catchments. This continuity between sites may indicate the sites share an upstream source contributing to low visual clarity (high turbidity).

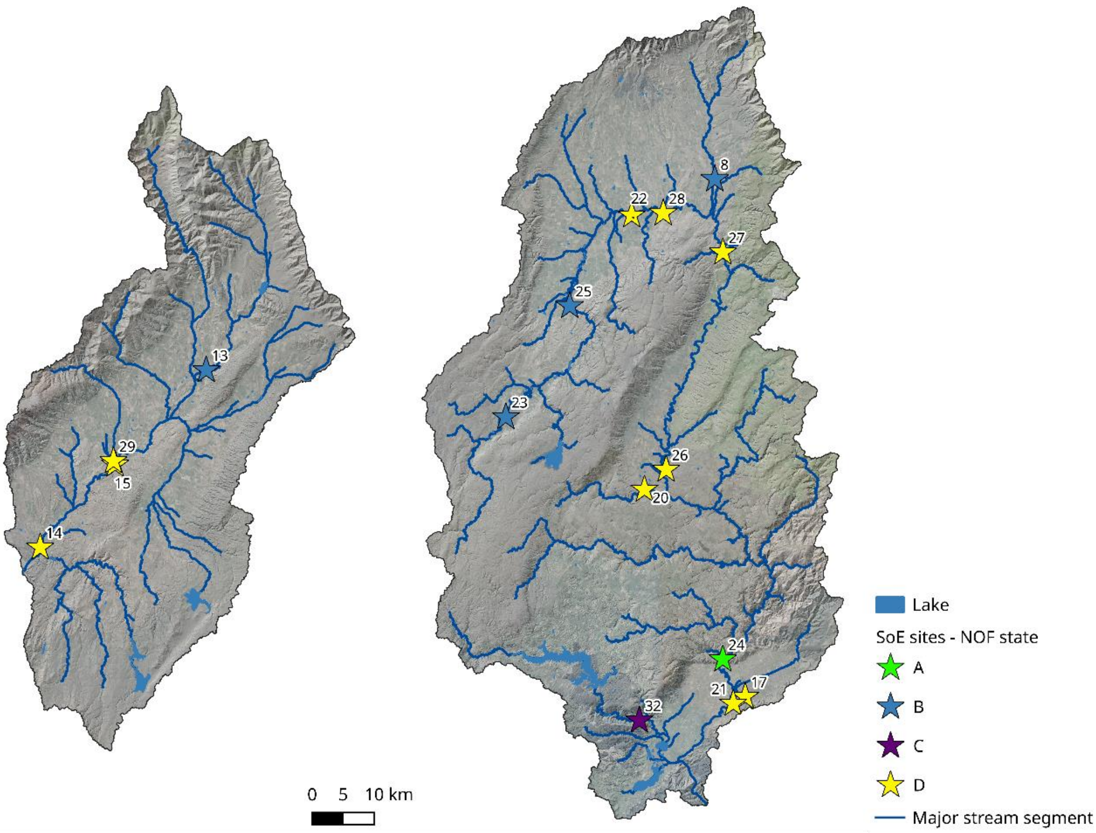

Figure 10. Demonstration of the continuity between non-compliant sites in the Manuherikia (left) and Taieri (right) catchments.

Low baseline visual clarity at these sites may also be attributable to non-sediment sources. Point source discharges such as effluent and sewage have been documented to occur in the Taieri catchment (ORC 2003, 2004) and may impact visual clarity. Bright & Mager (2016) note the potential for dissolved organic matter, such as tannins, to impact turbidity measurements (and therefore derived visual clarity). Tannins are a widely documented cause of water discolouration in Otago rivers and streams, such as in the Taieri catchment (ORC 2003, 2004; Uytendaal & Ozanne n.d.).

In cases where high turbidity measurements (low visual clarity) are attributable to naturally occurring processes which make the national bottom line unachievable, the NPS-FM 2020 allows for a target attribute state to be set below the national bottom line. In the case of suspended fine sediment, such natural processes may include naturally highly coloured brown-water streams (such as those impacted by tannins), streams affected by glacial flour, and selected lake-fed REC classes which may be impacted by autochthonous phytoplankton production. Further investigation is warranted to assess whether these exceptions apply to SoE sites in the Otago region.

6.3 Model assumptions and limitations

There are several limitations in the SedNetNZ modelling, and in the calculation of the load reductions required to meet NOF suspended fine sediment attribute states, that tend to relate to limitations associated with input data. We outline these limitations in terms of each modelling component below. Model outputs should be interpreted in the context of these limitations.

6.3.1 Surficial erosion

The key limitations in the surficial erosion component of SedNetNZ relate to the calculation of the *C* and *K* factors in the NZUSLE, and the availability of suitable input data. We have improved the calculation of the *K* factor within the Otago region by computing a spatially variable *K* factor instead of the uniform *K* factor previously used in the NZUSLE (e.g. Dymond et al. 2016). Higher resolution soils data from the region, such as S-map, may improve estimates of surficial erosion within Otago.

We have also improved the spatial distribution of the *C* factor by including winter forage cropping as a distinct land class in the NZUSLE. However, mapped locations of winter forage paddocks were only available in hill country. This at least captures the winter forage paddocks most prone to surficial erosion (steeper slopes). This component could be improved with region-wide mapping of winter forage paddocks.

6.3.2 Riverbank erosion

In the absence of local data on reach-scale bank migration rates, it was necessary to calibrate the bank migration model using available measurements from the Manawatū and Kaipara catchments in the North Island. We recognise this potentially introduces additional error into model predictions for Otago catchments due to differences in catchment geology and channel planform. However, the data from Manawatū and Kaipara do span a large range in observed bank migration rates, riparian woody vegetation extents, soil textures, channel slope, and sinuosity variables for the mapped reaches (Spiekermann et al. 2017; Smith et al. 2019a).

Representation of riparian woody vegetation has been derived from EcoSat Woody (Dymond & Shepard 2004) as LCDB is less suitable for representing narrow corridors of woody vegetation often found along channel banks. Predictions of bank migration rates are therefore based on this high-resolution mapping of woody vegetation presence/absence in 2002. A further challenge results from the spatial correspondence of mapped channel location and woody vegetation resulting from the alignment of REC2 to the channel, and changes in channel planform since mapping occurred. Availability of catchment-wide LiDAR data would enable improved representation of riparian woody vegetation and its spatial coherence with channel locations.

6.3.3 Extent of riparian fencing

The extent of fencing implemented in 2017 is a critical parameter for the model as this determines the remaining length of stream segments able to be fenced in the aspirational scenario. Due to a lack of spatial data on the location and extent of fencing in the Otago region, the Survey of Rural Decision Makers (SRDM) was used to estimate the extent of riparian fencing implemented in 2017. The SRDM asks respondents what proportion of major and minor streams they have fenced on their farms, but the 2017 survey did not ask whether they had minor or major streams present. This leads to some uncertainty around what proportion of major and minor streams have been fenced in the region. The 2021 SRDM did ask whether minor and major streams were present, and provides similar estimates of fencing to the 2017 SRDM, suggesting the 2017 survey gives a reasonable estimate of fencing proportions despite this limitation.

Some districts also had a low number of respondents for the SRDM, such as Queenstown-Lakes District and Dunedin City, and therefore results are based on a small sample of farmers and may not be representative of the true extent of fencing in the district. This uncertainty has less impact in the Queenstown-Lakes District as a significant proportion of the sediment generated from mitigatable land in this district is intercepted by lakes which buffer the effect of mitigation on downstream reaches. The district also comprises significantly less mitigatable land, and only one SoE site that does not meet the bottom line for suspended fine sediment, so the uncertainty in estimating the baseline extent of fencing in the Queenstown-Lakes District will have less impact on the results than it would in other districts.

Errors in the location of the REC2 network relative to the true location of the stream, and limitations with the mapping resolution of LCDB, may lead to misalignment between the location of the channel and mitigatable land, particularly in low order streams. This may contribute some error in the lengths of riparian fencing being assigned to any given REC2 segment. This error could be improved through production of a digital channel network derived from a higher-resolution LiDAR-based DEM, and higher resolution land cover and land use mapping.

The model has assumed all stream segments intersecting mitigatable land classes are suitable for fencing. However, some of these segments intersect steep land that may be deemed unsuitable for riparian fencing. The model may therefore over-estimate the extent of fencing which can be feasibly implemented in the aspirational scenario.

6.3.4 Required load reductions and achievable attribute states

There are several sources of uncertainty in the model which contribute to uncertainty in the calculations of suspended sediment load reductions required to meet NOF attribute states.

First, the visual clarity baselines at SoE sites were estimated from turbidity measurements using Franklin et al.'s (2019) relationship between turbidity and visual clarity calibrated on a national dataset (ORC, pers. comm., 27 April 2021.). Franklin et al. (2019) note the relationship between turbidity and visual clarity is often site-specific, and using a nationally fitted relationship to convert turbidity to visual clarity at a site may not be robust. Davies-Colley et al. (2021) and Davies-Colley & Smith (2001) have also highlighted issues related to the uncertainty in turbidity measurements, and the challenges of comparing turbidity between sites and instruments. These sources of uncertainty may lead to increased errors in the estimation of baseline visual clarity, misclassification of the baseline attribute state of a site, and errors in the reductions in load required to achieve visual clarity objectives. Developing site-specific relationships between turbidity and visual clarity and using these to calculate baseline attribute states would reduce this uncertainty.

Required load reductions have been estimated using empirical models relating improvements in visual clarity to reductions in suspended sediment load fitted to a national dataset (including sites from Otago, see Hicks et al. 2019). This should result in the models being fitted to a wide range of catchment variables and therefore representing the variability across Otago, but this may lead to under- or over-estimation of required reductions at any one site. This relationship does not account for the local variability in the relationship between suspended sediment load and visual clarity that arises due to variations in the sediment characteristics that affect the optical properties of flows between sites, such as the presence of fine-grained clay minerals (Hicks et al. 2019). This is particularly relevant for catchments with glacial sources of flow. Catchments with a predominantly glacial source of flow were excluded from our analysis. This relationship assumes visual clarity is primarily affected by suspended sediment and does not account for the potential influence of other matter, such as tannins, on visual clarity.

The relationship between suspended sediment load and flow has been assumed to remain constant at a site. However, this relationship may change due to changes in catchment hydrology resulting from changes in catchment land cover, land use, and climate, leading to changes in the relationship between a given flow and suspended sediment concentration (Hicks et al. 2019). As data are not presently available to predict these changes, we assume that the associated relationships remain constant across scenarios.

Visual clarity baseline attribute states are derived from monthly fixed interval turbidity measurements. Fixed interval sampling likely results in turbidity predominantly being measured at or near baseflow, when most of the suspended sediment load may be derived from within-channel sources (e.g. remobilisation from channel bed or from bank erosion). In contrast, the modelled mean annual suspended sediment loads also capture storm event-driven erosion and sediment loads. Hence, the link between reductions in storm-generated sediment loads and increases in visual clarity at generally low flows may depend in part on a reduction in the storage and subsequent remobilisation of storm-derived fine sediment in the channel network.

Climate change is expected to affect soil erosion and alter fine sediment loads entering rivers and coastal receiving environments (Basher et al. 2020; Vale et al. 2021), and may offset the impact of erosion control mitigations (Basher et al. 2020). The effects of climate change have not been included in the SedNetNZ scenarios for the Otago region. Future scenario modelling using SedNetNZ could represent the impacts of climate change on erosion and suspended sediment loads and assess the impact on the achievability of attribute states.

7 Conclusions

Under the baseline scenario, 489 kt yr^{-1} of suspended fine sediment was estimated to reach coastal receiving environments in Otago. Implementation of aspirational mitigations are modelled to achieve a 28% reduction in suspended sediment, resulting in 351 kt yr^{-1} reaching coastal receiving environments.

This reduction in suspended sediment load results in 12 of the 24 (50%) SoE sites with a baseline attribute state in the D band being brought above the national bottom line in the aspirational scenario. A further six SoE sites achieve both band A and band B under the aspirational scenario. In total, 49 of 61 sites (80%) comply with the national bottom line under the aspirational scenario compared with 37 (60%) at baseline.

Under the modelled aspirational mitigation scenario, 12 sites remain in band D. Further investigations into the contribution of dissolved organic matter to turbidity measurements at these sites would strengthen assessments of achievable attribute states. Where naturally occurring processes, such as the transport of tannins and high levels of dissolved organic matter, contribute to low visual clarity at these sites, objectives for suspended fine sediment may need to be set below the national bottom line in accordance with the NPS-FM 2020.

8 Recommendations

Future work could adopt the following recommendations to improve representation of erosion and sediment delivery processes and the assessment of mitigation measures required to achieve suspended fine sediment objectives in Otago:

- Acquisition of spatial data on the extent of existing riparian fencing across the region would enable a) better parameterisation of the baseline scenario, and b) more accurate estimation of the remaining length of streams to be fenced under future mitigation scenarios.
- Future suspended sediment load modelling could include representation of the potential impacts of climate change on the achievability of attribute states.
- Use of LiDAR data would support improved representation of erosion processes. SedNetNZ modelling could be updated when LiDAR data become available for the Otago region.
- Investigations into the influence of dissolved organic matter on turbidity would improve the ability to estimate achievable attribute states for suspended fine sediment in the Otago region and set feasible objectives.

9 Acknowledgements

We thank Otago Regional Council for funding this work. We acknowledge staff from Otago Regional Council, particularly Rachel Ozanne, Helen Manly, and Jason Augspurger for discussions leading to this piece of work, and for provision of data. We thank Chris Philips for reviewing this report.

10 References

Abernethy B, Rutherfurd ID 2000. The effect of riparian tree roots on the mass-stability of riverbanks. Earth Surface Processes and Landforms 25: 921–937.

Alber A, Piégay H 2017. Characterizing and modelling river channel migration rates at a regional scale: case study of south-east France. Journal of Environmental Management 202: 479–493.

Arulanandan K, Gillogley E, Tully R 1980. Development of a quantitative method to predict critical shear stress and rate of erosion of natural undisturbed cohesive soils. USACE, Waterways Experiment Station Technical Report GL-80-5. Vicksburg, MS: USACE.

Basher L, Spiekermann R, Dymond J, Herzig A, Hayman E, Ausseil AG 2020. Modelling the effect of land management interventions and climate change on sediment loads in the Manawatū–Whanganui region. New Zealand Journal of Marine and Freshwater Research 2020 54: 490–511.

Belliss SE, Pairman D, Dymond J, Amies A, Zoerner J, Shepherd J, Drewry J, North H 2019. Identification of high-risk agricultural activities: national mapping of the location, scale and extent of winter forage cropping and intensive grazing on hill country land. Manaaki Whenua - Landcare Research Contract Report LC3469 prepared for Ministry for the Environment.

Bright CE, Mager SM 2016. Contribution of particulate organic matter to riverine suspended material in the Glendhu experimental catchments, Otago, New Zealand. Journal of Hydrology (NZ) 55: 89–105.

Brune GM 1953. Trap efficiency of reservoirs. Eos, Transactions American Geophysical Union 34: 407–18.

Crosato A 2009. Physical explanations of variations in river meander migration rates from model comparison. Earth Surface Processes and Landforms 34: 2078–2086.

Davies-Colley, R, Hughes, AO, Vincent, AG, Heubeck, S 2021. Weak numerical comparability of ISO-7027-compliant nephelometers. Ramifications for turbidity measurement applications. Hydrological Processes 35(12): e14399.

Davies-Colley RJ, Smith DG 2001. Turbidity suspended sediment, and water clarity: a review. JAWRA Journal of the American Water Resources Association 37: 1085–1101.

De Rose R, Basher LR 2011. Measurement of river bank and cliff erosion from sequential LiDAR and historical aerial photography. Geomorphology 126: 132–147.

De Rose R, Prosser IP, Weisse M, Hughes AO 2003. Patterns of erosion and sediment and nutrient transport in the Murray-Darling Basin. CSIRO Land and Water Technical Report 32/03.

Desmet PJJ, Govers G 1996. A GIS procedure for automatically calculating the USLE LS factor on topographically complex landscape units. Journal of Soil and Water Conservation 51(5): 427–433.

Dunn IS 1959. Tractive resistance of cohesive channels. Journal of the Soil Mechanics and Foundations Division 85: 1–24.

Dymond JR, Betts HD, Schierlitz CS 2010. An erosion model for evaluating regional land-use scenarios. Environmental Modelling and Software 25: 289–298.

Dymond JR, Davies-Colley RJ, Hughes AO, Matthaei CD 2017. Predicting improved optical water quality in rivers resulting from soil conservation actions on land. Science of the Total Environment 603–604: 584–592.

Dymond JR, Herzig A, Basher L, Betts HD, Marden M, Phillips CJ, Ausseil AE, Palmer DJ, Clark M, Roygard J 2016. Development of a New Zealand SedNet model for assessment of catchment-wide soil-conservation works. Geomorphology 257: 85–93.

Dymond JR, Shepherd JD 2004. The spatial distribution of indigenous forest and its composition in the Wellington region, New Zealand, from ETM+ satellite imagery. Remote Sensing of Environment 90: 116–125.

Elliott A, Semadeni-Davies AF, Shankar U, Zeldis JR, Wheeler DM, Plew DR, Rys GJ, Harris SR 2016. A national-scale GIS-based system for modelling impacts of land use on water quality. Environmental Modelling & Software. 86: 131–144.

Foster GR, Meyer LD, Onstad CA 1977. A runoff erosivity factor and variable slope length exponents for soil loss estimates. Transactions of the ASAE 20: 683–687.

Franklin P, Stoffells R, Clapcott J, Booker D, Wagenhoff A, Hickey C 2019. Deriving potential fine sediment attribute thresholds for the National Objectives Framework. NIWA Client Report 2019039HN prepared for Ministry for the Environment.

Fryirs KA, Wheaton JM, Brierley GJ 2016. An approach for measuring confinement and assessing the influence of valley setting on river forms and processes. Earth Surface Processes & Landforms 41: 701–710.

Gill MA 1979. Sedimentation and useful life of reservoirs. Journal of Hydrology 44: 89–95.

Hall JE, Holzer DM, Beechie TJ 2007. Predicting river floodplain and lateral channel migration for salmon habitat conservation. Journal of the American Water Resources Association 43: 786–797.

Hanson GJ, Simon A 2001. Erodibility of cohesive streambeds in the loess area of the midwestern USA. Hydrological Processes 15: 23–38.

Hickin EJ, Nanson GC 1984. Lateral migration rates of river bends. Journal of Hydraulic Engineering 110: 1557–1567.

Hicks M, Haddadchi A, Whitehead A, Shankar U 2019. Sediment load reductions to meet suspended and deposited sediment thresholds. NIWA Client Report 2019100CH prepared for Ministry for the Environment.

Hicks DM, Shankar U 2020. Technical report 6: Sediment load reduction load reduction to meet visual clarity bottom lines. NIWA memo prepared for MfE. Available from https://environment.govt.nz/assets/publications/Files/technical-report-6-sediment-load-reductions-to-meet-visual-clarity-bottom-lines.pdf

Hooke JM 1979. An analysis of the processes of river bank erosion. Journal of Hydrology 42: 39–62.

Hubble TCT, Docker BB, Rutherfurd ID 2010. The role of riparian trees in maintaining riverbank stability: a review of Australian experience and practice. Ecological Engineering 36: 292–304.

Hughes AO, Prosser IP 2003. Gully and riverbank erosion mapping for the Murray-Darling Basin. CSIRO Land and Water Technical Report 3/03.

Julian JP, Torres R 2006. Hydraulic erosion of cohesive riverbanks. Geomorphology 76: 193–206.

Konsoer KM, Rhoads BL, Langendoen EJ, Best JL, Ursic ME, Abad JD, Garcia MH 2015. Spatial variability in bank resistance to erosion on a large meandering, mixed bedrock-alluvial river. Geomorphology 252: 80–97.

McCool DK, Foster GR, Mutchler CK, Meyer LD 1989. Revised slope length factor for the Universal Soil Loss Equation. Transactions of the ASA 32: 1571-76.

Monaghan R, Manderson A, Basher L, Spiekermann R, Dymond J, Smith C, Muirhead R, Burger D, McDowell R 2021. Quantifying contaminant losses to water from pastoral landuses in New Zealand II. The effects of some farm mitigation actions over the past two decades. New Zealand Journal of Agricultural Research 0: 1–25.

Nanson GC, Hicken EJ 1983. Channel migration and incision on the Beatton River. Journal of Hydraulic Engineering 109: 327–337.

Nanson GC, Hickin EJ 1986. A statistical analysis of bank erosion and channel migration in western Canada. Geological Society of America Bulletin 97: 497–504.

Neverman AJ, Djanibekov U, Soliman T, Walsh P, Spiekermann R, Basher L 2019. Impact testing of a proposed suspended sediment attribute: identifying erosion and sediment control mitigations to meet proposed sediment attribute bottom lines and the costs and benefits of those mitigations. Manaaki Whenua – Landcare Research Contract Report LC3574 prepared for Ministry for the Environment.

Neverman A, Smith HG, Herzig A 2021a. Planning soil conservation for sediment load reduction in Taranaki. Manaaki Whenua – Landcare Research Contract Report LC3942 prepared for Taranaki Regional Council.

Neverman A, Smith HG, Herzig A, Basher L 2021b. Modelling baseline suspended sediment loads and load reductions required to achieve Draft Freshwater Objectives for Southland. Manaaki Whenua – Landcare Research Contract Report LC3749 prepared for Environment Southland.

Newsome PFJ, Wilde RH, Willoughby EJ 2008. Land resource information system spatial data layers: data dictionary. Palmerston North: Landcare Research New Zealand Ltd. http://digitallibrary.landcareresearch.co.nz/cdm/ref/collection/p20022coll14/id/67

Otago Regional Council (ORC) 2003. Report on the surface water quality of the Upper Taieri River Catchment, November 2001 to December 2002. ISBN 1-877265-30-6.

Otago Regional Council (ORC) 2004. Report on the surface water quality of the Lower Taieri River Catchment. ISBN 1-877265-32-2.

Polvi LE, Wohl E, Merritt DM 2014. Modeling the functional influence of vegetation type on streambank cohesion. Earth Surface Processes & Landforms 39: 1245–1258.

Renard KG 1997. Predicting soil erosion by water: a guide to conservation planning with the Revised Universal Soil Loss Equation (RUSLE). Washington DC: United States Government Printing.

Rosewell CJ, Loch RJ 2002. Estimation of the RUSLE soil erodibility factor. In: McKenzie N, Coughlan K, Cresswell H eds Soil physical measurement and interpretation for land evaluation. Melbourne, Australia: CSIRO Publishing.

Simon A, Collinson AJC 2002. Quantifying the mechanical and hydrologic effects of riparian vegetation on streambank stability. Earth Surface Processes & Landforms 27: 527–546.

Smith HG, Spiekermann R, Dymond J, Basher L 2019a. Predicting spatial patterns in riverbank erosion for catchment sediment budgets. New Zealand Journal of Marine and Freshwater Management 53: 338–362.

Smith HG, Herzig A, Dymond J, Basher L 2019b. Application of a revised SedNetNZ model to the Oreti and Aparima catchments, Southland. Manaaki Whenua – Landcare Research Contract Report LC3507 prepared for Our Land and Water National Science Challenge.

Smith HG, Spiekermann R, Herzig A, Dymond J 2020. Application of a revised bank erosion model to update SedNetNZ results for Hawke's Bay. Manaaki Whenua – Landcare Research Contract Report LC3740 prepared for Hawke's Bay Regional Council.

Spiekermann R, Betts H, Dymond J, Basher L 2017. Volumetric measurement of riverbank erosion from sequential historical aerial photography. Geomorphology 296: 193–208.

Stahlmann-Brown 2021. 'Survey of Rural Decision Makers'. Internet-based survey covering 6700 farmers, foresters, growers, and lifestyle block owners across New Zealand. Manaaki Whenua – Landcare Research. https://doi.org/10.7931/3tcs-wb24

Thorne CR 1990. Effects of vegetation on riverbank erosion and stability. In: Thornes JB ed. Vegetation and erosion. Chichester, UK: John Wiley & Sons. Pp. 125–144.

Trimble SW 1994. Erosional effects of cattle on streambanks in Tennessee, U.S.A. Earth Surface Process & Landforms 19: 451–464.

Uytendaal A, Ozanne R n.d. State of the Environment Surface Water Quality in Otago: 2006 to 2017. Dunedin: Otago Regional Council.

Vale S, Smith HG, Neverman A, Herzig A 2021. Application of SedNetNZ with erosion mitigation and climate change scenarios and temporal disaggregation in the Bay of Plenty Region. Manaaki Whenua – Landcare Research Contract Report LC4002 prepared for Bay of Plenty Regional Council.

Walker M, Rutherfurd ID 1999. An approach to predicting rates of bend migration in meandering alluvial streams. In: Rutherfurd ID, Bartley R eds Proceedings of the Second Australian Stream Management Conference. Melbourne, Australia: Cooperative Research Centre for Catchment Hydrology. Pp. 659–665.

Wang G, Gertner G, Xianzhong L, Anderson A 2001.Uncertainty assessment of soil erodibility factor for revised universal soil loss equation. Catena 46: 1–14.

Wilkinson SN, Olley JM, Prosser IP, Read IP. 2005. Targeting erosion control in large river systems using spatially distributed sediment budgets. In: Batalla RJ, Garcia C eds Geomorphological processes and human impacts in river basins. Wallingford: International Association of Hydrological Sciences Publ. No. 299. Pp. 56–64.

Wischmeier WH, Johnson CB, Cross BV 1971. Soil erodibility nomograph for farmland and construction sites. Journal of Soil and Water Conservation 26: 189193.

Woods R, Hendrikx J, Henderson R, Tait A 2006. Estimating mean flow of New Zealand rivers. Journal of Hydrology (NZ) 45: 95–110.

Wyn T, Mostaghimi S 2006. The effects of vegetation and soil type on streambank erosion, southwestern Virginia, USA. Journal of the American Water Resources Association 42: 69–82.

Yang X, Gray J, Chapman G, Zhu Q, Tulau M, McInnes-Clarke S 2018. Digital mapping of soil erodibility for water erosion in New South Wales, Australia. Soil Research 56: 15870.

Zhang X, Liu X, Zhang M, Dahlgren RA, Eitzel M 2010. A Review of vegetated buffers and a meta-analysis of their mitigation efficacy in reducing nonpoint source pollution. Journal of Environmental Quality 39(1): 76–84.